RICES

RESEARCH INNOVATION COMMERCIALISATION & ENTREPRENEURSHIP SHOWCASE

2020

ENGINEERING & INDUSTRIAL DESIGN

MMU MULTIMEDIA UNIVERSITY | PRESS

Published by
MMU Press
Research Management Centre
Multimedia University
2 nd Floor, Chancellery Building
Persiaran Multimedia
63100 Cyberjaya
Selangor Darul Ehsan

e-ISBN: 978-967-19560-3-8

Perpustakaan Negara Malaysia Cataloguing-in-Publication Data

Research Innovation Commercialisation & Entrepreneurship Showcase
(2020 : Online)
RICES 2020 : RESEARCH INNOVATION COMMERCIALISATION &
ENTREPRENEURSHIP SHOWCASE : ENGINEERING & INDUSTRIAL
DESIGN / editor Dr. Tan Yi Fei.
Mode of access: Internet
eISBN 978-967-19560-3-8
1. Education, Higher--Malaysia--Exhibitions.
2. Universities and colleges--Malaysia--Exhibitions.
3. Engineering--Exhibitions.
4. Industrial design--Exhibitions.
5. Electronic books.
I. Tan, Yi Fei, Dr. II. Title.
378.595

Cover design by Ms. Qistina Binti Ruslan.

RICES 2020 - ENGINEERING & INDUSTRIAL DESIGN

The publisher hereby records its gratitude to individuals who have helped in one way or another to make this book project a reality.

CONTENTS

FOREWORD

ENGINEERING & INDUSTRIAL DESIGN

FOREWORD

Vice President, RICES 2020

RICES 2020 is one of the numerous publications, including journals that MMU Press takes pride in. I am truly pleased that MMU Press have embarked on the initiative to publish this book.

Despite the global pandemic, the event RICES 2020 was successfully organised virtually, showcasing a multitude of exhibits reflecting research, innovation, commercialization and entrepreneurship activities and achievements. The RICES 2020 book is an extended compilation of MMU's researchers and entrepreneurs' fascinating insights on research ventures and idea creation for commercialising research output as well entrepreneurship. RICES is an excellent platform for MMU to interact with internal and external stakeholders. These interactions enable researchers to realise potentials for collaborations, IP exploitations, commercialisation and further research. It allows for industrial related viable research and feasible output. This RICES 2020 publication extends the present interactions even further, allowing for post-event interactions to materialise beyond the existing valued stakeholders.

RICES 2020 is evidence of the excellent effort by the RICES 2020 organisers and MMU Press. Their commitment and dedication have paid out with another hallmark achievement reflecting the division's synergy in the development of Research-Innovation- Commercialisation-Entrepreneurship (R-I-C-E) nexus in all research activities. I look forward to RICES 2020 publication.

Thank you.

Prof. Ir. Dr. Hairul Azhar bin Abdul Rashid
Vice President, Research and Industrial Collaboration and Engagement
Multimedia University

FOREWORD

Director, RICES 2020

On behalf of the Committee, it is my great pleasure to welcome you to RICES 2020, the fourth Research, Innovation, Commercialization, Entrepreneurship, Showcase. RICES is an annual event organized by Multimedia University to showcase research innovations, commercialization and entrepreneurship. RICES 2020, with the overarching theme of "Humanizing Innovation," is being held virtually on December 9-10, 2020, allowing for a borderless audience and safe interaction among inventors, venture capitalists, and industries in the midst of COVID-19. It is about ensuring that the results of research and innovation contribute to positive changes in people's lives, society, industry, and the country as a whole.

RICES 2020 pioneered the use of Virtual Reality technology to elevate the virtual exhibition experience by transforming in-person perspectives into an interactive and immersive virtual experience. For the first time, RICES 2020 hosted a virtual conference, disseminating the most recent research results and findings for researchers and academics to discuss. This year, 194 projects were accepted for presentation at RICES 2020, distributed across Project Showcase (Research Project, Social Innovation Project, and Startups), Embedding Entrepreneurial Learning, and Conference. Both internal and external judges who evaluated the showcases had used the judging criteria similar to those set for international exhibitions such as International Conference and Exposition on Inventions by Institutions of Higher Learning (PECIPTA) and International Invention, Innovation & Technology Exhibition (ITEX).

I would like to express my heartfelt gratitude to the organizing committee and everyone who helped make RICES 2020 a success in various ways. Last but not the least, I would like to thank everyone who submitted work and participated in RICES 2020.

Thank you all for contributing!

Mr. Cheong Soon Nyean
Director of RICES 2020
Deputy Director, Technology Transfer Office
Multimedia University

FOREWORD

Deputy Director, RMC
(Head, MMU PRESS)

I would like to humbly thank various people who made MMU Press publications a success especially in its RICES publications 2020. Congratulations to Mr. Cheong Soon Nyean, Director of RICES 2020 who has successfully organized the event despite the Covid-19 pandemic. The RICES 2020 hosted the Virtual Reality technology to ensure all participants and visitors immerse into this virtual experience and making the participation almost possible for everyone.

On top of that, RICES showcases the best technology, research innovation, R&I commercialization, receives valuable feedback and develops new partnerships that bring great value to society. MMU Press is proud to have produced a total of 5 publications in 2021 namely research on (i) Engineering, (ii) ICT and Multimedia (iii) Social Science, (iv) Entrepreneurship & Social innovation projects as well as (v) RICES Conference Extended Abstract.

It is our utmost hope that MMU Press mission will be an internationally recognized academic press. Its spirit is to connect Multimedia University (MMU) with the larger communities and institution through innovative and inspiring writings. We welcome all contributors to publish with MMU Press to better equip ourselves and the community at large with various new ideas and technologies.

Finally, all these achievements are made possible due to strong commitment by all especially the Coordinator of Special Publication – Dr. Tan Yi Fei, chief editors, editorial team members and the project leaders, who have contributed to the publication of RICES 2020. Kudos to all of you! Thank you and let's make MMU Press be the beacon of knowledge.

Assoc. Prof. Dr. Tan Siow Hooi
Deputy Director, Research Management Centre (Head, MMU Press)
Multimedia University

ENGINEERING & INDUSTRIAL DESIGN

MMU® MULTIMEDIA UNIVERSITY | PRESS

A STUDY ON BRAIN ACTIVITY DURING QURAN LISTENING AND RECITATION

Team members: Ms. Nur Asyiqin binti Amir Hamzah, Ms. Nur Hasanah binti Ali, Ms. Noor Ziela binti Abd Rahman, Dr. Ervina Efzan binti Mhd Noor & Dr. Azlan bin Abd Aziz | FET MMU
Research assistants: Mohamad Razwan bin Abdul Malek & Muhamad Razlan bin Kamaruzaman | FET MMU
Funds: Fisabilillah Research & Development Grant Scheme (FRDGS)

Brainwaves are produced by synchronised electrical pulses from masses of neurons communicating with each other. In this research, we analysed the waves produced by the brain (EEG) when listening and reciting Quran. EEG signal was extracted from the brain using Emotiv EPOC. The experiment consists of two parts; reading and listening. Participants were requested to read and listen to two surahs that were pre-determined. Next, classification of the waves into positive or negative category was conducted.

METHODOLOGY

Research Flowchart

1 Systematic Literature Review
2 Data Collection
3 Data Classification
4 Analysis & Conclusion

Systematic Literature Review

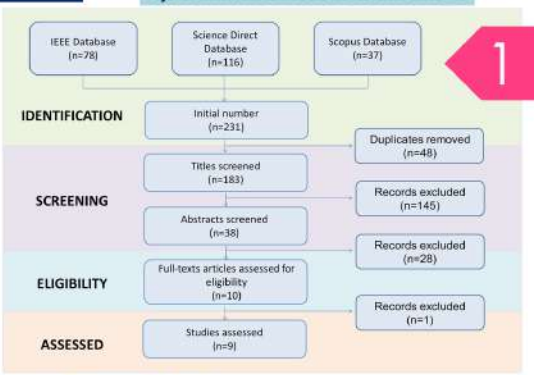

Research Gap:
- Small dataset
- Unclear reason of the selected Surahs

2

1 Sit properly on a chair
2 Relax for 1 minute (eyes closed)
3 Listen to Quran (eyes closed)
4 Relax for 2 minutes (eyes opened)
5 Recite Quran for 2 minutes
6 Relax for 1 minute

3

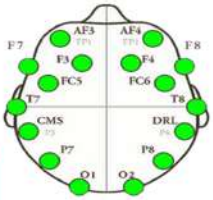

CONCLUSION

4

Listening
- Stress
- Engagement
- Interest

Conclusion
- **Stress:** Fear to the punishment of the hell
- **Engagement & interest:** Curiosity to know about the power and sustenance of Allah SWT

Reciting
- Stress
- Engagement
- Interest
- Focus

Conclusion
- **Stress:** Fear of destruction of the disbelievers took as they disobeyed Allah SWT
- **Engagement, interest & focus:** Curiosity of people who lived in the ancient time

Participant Info	Listening (Al-Fajr)	Reciting (Al-Mulk)
• Total: 50 person • Age: 19-24 years old • Gender: Male	**Content:** Destruction of disbelieving peoples; the Ancient Egyptians, the people of Iram of the Pillars and Mada'in Saleh. **Reason of selection:** Short and easy to recite surah	**Content:** The power and sustenance of the Almighty so evident in this universe bears evidence that those who deny the Day of Reward and Punishment will have to face the torment of hell. **Reason of selection:** Familiar and common surah

AWARD & PUBLICATION
- Silver Award: RICES2019
- Poster published: eRICES2019
- Journal submitted: Inderscience Publication

ALICE: A General-Purpose Framework for a Virtual Artificial Intelligent Agent

Dr Ooi Chee Pun, Dr Tan Wooi Haw, Dr Tan Yi Fei, Quek Albert, Poh Soon Chang, Yap Zhun Hau

Introduction

- There exist two types of virtual assistants: text-based chatbots and voice assistants.
- Voice assistants such as Alexa and Siri provide more natural conversation.
- However, they appear apathetic compared to human conversation.
- Our research aims to reduce this gap.
- We introduced a virtual assistant which combines 3D avatar, face detection, face recognition and face expression recognition with voice assistant.

Methodology

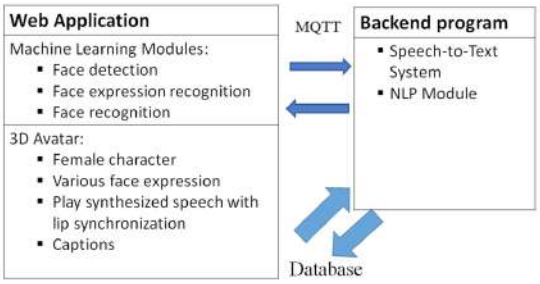

- Two main parts: Web application and backend program.
- Run both programs on computer with webcam.
- Web application consists of machine learning models and 3D avatar, run on WAMP server.
- Machine learning models:

1. Face detection: Detect the location of face in images.
2. Face recognition: Identify the identity of the faces.
3. Face expression recognition: Detect the facial expression of human users.

- 3D avatar:

❑ Female character called Alice.
❑ Various face expressions such as happy, sad and furious.

❑ Synthesized speech from text using Google Text-to-Speech service.
❑ Lip synchronized with the audio.
❑ Captions provided.

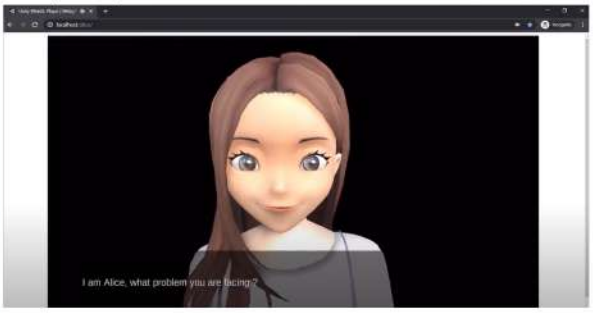

Backend Program

- Speech recognition to convert human speech into text using Google Speech-to-Text service.
- Natural Language Processing (NLP) to analyze and understand the text transcript.
- Combining 2 methods of NLP:

1. Use deep learning to classify the texts into different classes such as *Upgrading*, *Payment*, *Device Malfunction*, *Internet outage* and *Unknown* class.
2. If the text is classified as *Unknown*, we will search for pre-defined keywords in the texts.

- Once the intent of the text is detected, the program sends a MQTT command to web application to tell which audio file to be played.
- The web application also passes the identity of the human user.
- The backend program can access the database to retrieve the user's personal information and history.

Proof of Concept Demo

- Customer Service Agent
- Question Answering

MULTIMEDIA UNIVERSITY

ARTIFICIAL NEURAL NETWORK MODELLING OF 3D PRINTED PLA PART

Clement Rao Thomas, Dr. Chockalingam Palanisamy

Introduction

The worldwide market and suppliers have been searching for ways to produce quality products at reduced costs. The objective of this research is to develop an Artificial Neural Network model to predict the strength of a 3D printed PLA part.

Methods & Materials

Design of Experiment (DOE), Central Composite Design (CCD) (Fig. 1), with three input parameters (Table 1) ie., layer thickness, Infill density and number of shells with three levels were used in this investigation. Based on the CCD Design Matrix (Table 2), 15 sets of samples were 3D printed using Makerbot Replicator with PLA material. Tensile, Hardness and Compression Testing were carried out on the samples and data was recorded. Using the data, an Artificial Neural Network model was created using the Neural Network Toolbox in Matlab.

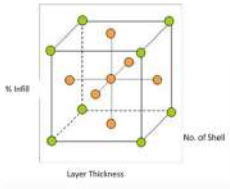

Figure 1 Central Composite Design (CCD)

Table 1 Input Parameters and Levels

Parameter	Levels		
	-1	0	1
Layer thickness	0.1	0.2	0.3
Infill density	15	30	60
Number of shells	2	3	4

Table 2 CCD Design Matrix

Test Number	Coded values			Actual values		
No.	Layer Thickness	Number of Shells	Infill Density	Layer Thickness (mm)	Number of Shells	Infill Density (%)
1	-1	-1	-1	0.1	2	15
2	1	-1	-1	0.3	2	15
3	-1	1	-1	0.1	4	15
4	1	1	-1	0.3	4	15
5	-1	-1	1	0.1	2	60
6	1	-1	1	0.3	2	60
7	-1	1	1	0.1	4	60
8	1	1	1	0.3	4	60
9	-1	0	0	0.1	3	30
10	1	0	0	0.3	3	30
11	0	-1	0	0.2	2	30
12	0	1	0	0.2	4	30
13	0	0	-1	0.2	3	15
14	0	0	1	0.2	3	30
15	0	0	0	0.2	3	30

Results & Discussion

Figure 2 (a), (b) and (c) show the mechanical test results from the experiments. Using the experimental data, an artificial neural network model is created. The created model is validated and adopted for prediction of new data. Artificial Neural Network Model was used to predict output for five new sets of input parameters. Then using the same input parameters, sample parts were printed and actual mechanical strength of the parts were experimentally found out. The percentage differences between the values are below 5%. These results validate the developed ANN model for prediction of mechanical strengths.

Figure 2 (a) Tensile Test (b) Compression Test (c) Hardness Test

Parameter range Number	Layer thickness (0.1-0.3)	Number of shells (2-4)	Infill density (15-60)	Tensile Test, N (ANN Modelling)	Printed Modelling Parameters after testing, N	Percentage difference (%)
1	0.13	2	20	1211.1	1210.893	5
2	0.16	2	25	1462.68	1460.970	3.9
3	0.19	3	30	1815.6	1809.586	3
4	0.22	3	35	1847.5	1860.886	4.1
5	0.25	4	40	1801.6	1147.650	3

Parameter range Number	Layer thickness (0.1-0.3)	Number of shells (2-4)	Infill density (15-60)	Compression Test, KN (ANN Modelling)	Printed Modelling Parameters after testing, kN	Percentage difference (%)
1	0.13	2	20	13.7135	14.3991	4.9
2	0.16	2	25	9.7395	10.2264	4.89
3	0.19	3	30	11.5682	12.0226	3.93
4	0.22	3	35	7.8344	8.14777	3.88
5	0.25	4	40	7.6555	7.96172	4

Parameter range Number	Layer thickness (0.1-0.3)	Number of shells (2-4)	Infill density (15-60)	Hardness Test, (ANN Modelling)	Printed Modelling Parameters after testing	Percentage difference (%)
1	0.13	2	20	53.8813	56.9515	4.9
2	0.16	2	25	53.5883	55.6486	3.9
3	0.19	3	30	70.7451	73.0474	3
4	0.22	3	35	50.5811	52.0085	3
5	0.25	4	40	43.2249	44.5216	3.2

Table 3 ANN predicted data and 3D printed sample parts experimental data (a) Tensile, (b) Compression, (c) Hardness.

Conclusion

Sample parts with different combination of input parameters were printed and tested for mechanical strengths. Using the data, an ANN model is created and validated. The model was used to predict the mechanical strength of the 3D printed parts for new set of input parameters. Using the same input parameters, new sample parts were printed and tested for mechanical strengths. The ANN predicted data and experimental data were compared. There were only 5% of variations between the data. This validates the developed model and enables its use to predict the mechanical strength of 3D printed parts.

Comparison of Modelling Techniques for Polymer Fiber Drawing Systems

Project Leader: Dr. Cham Chin Leei
Project Members: Assoc. Prof. Dr. Tan Ai Hui
Prof. Zulfadzli Yusoff

Introduction:

- Fiber drawing system describes filament extrusion that has been drawn down post-extrusion. Mathematical modelling for fiber drawing system describes mathematical description of the characteristic that the fiber has made thinner in diameter as a result of the drawing process.

Methods & Materials:

- In the melting phase, the polymer chains are arranged in a random or disorder state, the extrusion process initiates orientation of the chain in the extrusion direction. Several modelling protocols are being used to compare the effects of input such as temperature, humidity, air pressure and godet rolls which resulted in varying output of the drawn fiber.

Results:

- Nonlinear MIMO models could describe the fiber drawing process with minimum error. From the selected model, an optimal controller could be designed to perform the polymer fiber drawing system.

Discussion:

- The fundamentals provide a framework to explain the properties of the polymer fiber drawing process by using mathematical models. Researchers can tweet and twist the parameters of the fiber drawing process, continue to improve and enhance the techniques.

Conclusions:

- Fiber drawing static and dynamic characteristics are measured and compared with experimental published data. A detailed experimental setup and procedure for both cases are presented. The comparison of the results show a very good agreement with static drawn parameters and dynamic drawn coefficients while there is a small difference in the dynamic drawn coefficient, which may be due to the varying season during the experimental period.

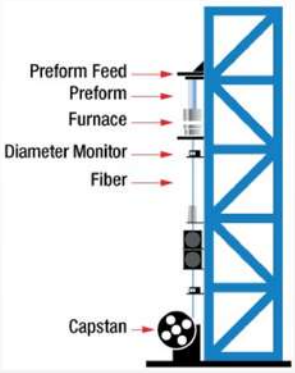

Fig 1: Polymer fiber drawing tower concept

Fig 2: Polymer fiber drawing tower in the lab

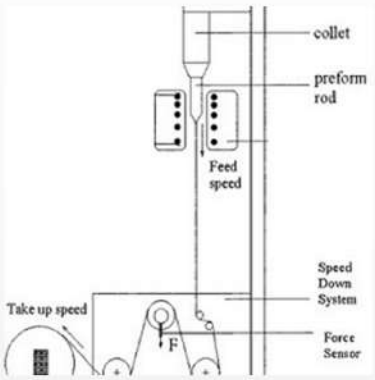

Fig 3: Modelling of Polymer fiber drawing tower

COV-CTX: LUNG CT SCANS and X-RAYS ARTIFICIAL INTELLIGENCE ENABLED ANALYZER for COVID-19 CASES

Nor Azlina Binti Ab. Aziz[a], Md Armanur Rahman[a], Chy Mohammed Tawsif Khan[a], Sharifah Noor Masidayu Binti Sayed Ismail[b], Siti Zainab Ibrahim[b], Nor Hidayati Abdul Aziz[a], Md Jakir Hossen[a], Syabeela Syahali[a], Muharniza Azinita Musa[a], Nor Hidayah Mohamad[a], Kamarulzaman Ab Aziz[c]

[a]Faculty of Engineering & Technology, [b]Faculty of Information Science & Technology, [c]Faculty of Management, Multimedia University

Introduction

The world is in turmoil with the outbreak of COVID-19 pandemic. By 17 Nov 2020, a year after the virus was first reported in Wuhan, China, more than 54.7million cases are confirmed with more than 1.3million deaths worldwide as reported by WHO. Numerous research works are conducted globally to help combat this pandemic. Most COVID-19 patients are reported to have lung-related problems. Therefore, the usage of lungs' X-rays and CT scans had been proposed to facilitate screening of COVID-19 patients. In June 2020, the WHO had suggested the usage of chest imaging for patients of from the following four categories:

R2.2 For symptomatic patients with suspected COVID-19, WHO suggests using chest imaging for the diagnostic workup of COVID-19 when: (1) RT-PCR testing is not available; (2) RT-PCR testing is available, but results are delayed; and (3) initial RT-PCR testing is negative, but with high clinical suspicion of COVID-19.

Conditional recommendation, based on low certainty evidence

R3 For patients with suspected or confirmed COVID-19, not currently hospitalized and with mild symptoms, WHO suggests using chest imaging in addition to clinical and laboratory assessment to decide on hospital admission versus home discharge.

Conditional recommendation, based on expert opinion

R4 For patients with suspected or confirmed COVID-19, not currently hospitalized and with moderate to severe symptoms, WHO suggests using chest imaging in addition to clinical and laboratory assessment to decide on regular ward admission versus intensive care unit (ICU) admission.

Conditional recommendation, based on very low certainty evidence

R5 For patients with suspected or confirmed COVID-19, currently hospitalized and with moderate to severe symptoms, WHO suggests using chest imaging in addition to clinical and laboratory assessment to inform therapeutic management.

Conditional recommendation, based on very low certainty evidence

Figure 1: Recommendations on the use of chest imaging in the diagnostic workup and clinical management of patients with COVID-19 by World Health Organization (2020)

This project utilized Artificial Intelligence (AI) technology to detect COVID-19 patients using chest images as per WHO recommendations. Specifically, the COV-CTX system is using deep learning to analyze X-rays and CT scans chest images of symptomatic patients for sign of COVID-19 infection. This is done without the need of human-assistance. The image analysis accuracy rate of COV-CTX is at 97%.

Research Methodology

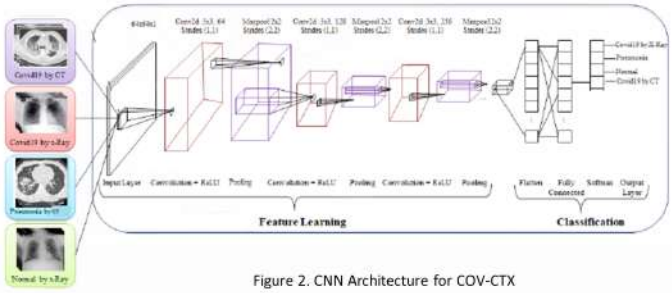

Figure 2. CNN Architecture for COV-CTX

Result of COV-CTX

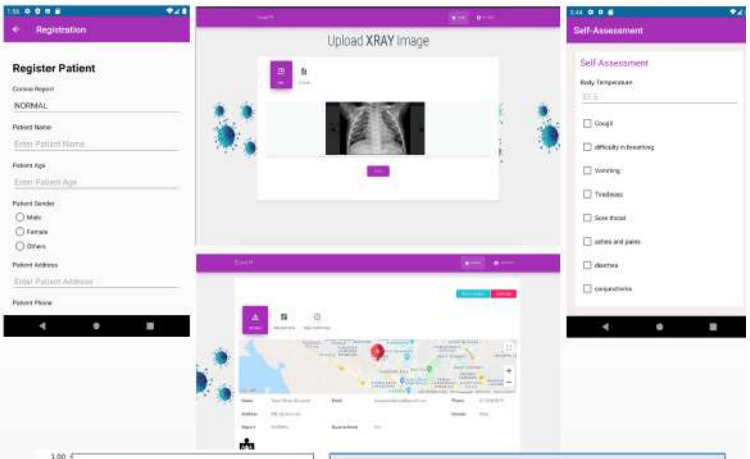

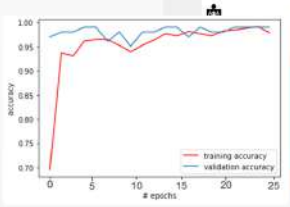

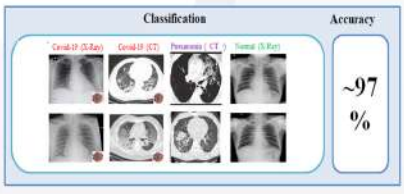

Conclusion

COVID-19 frequently affects the lung cells. In this study, the Deep CNN algorithm was employed to detect the COVID-19 using chest images, particularly the lung CT scans and X-rays. The classification accuracy achieved reach 97%. A web-based and Android mobile application were developed for COV-CTX. Furthermore, the system was designed as a holistic solution that also incorporate telehealth, patients management and tracking system that can help authorities better address this pandemic.

Life Made Easier™ | TM Group

DATA ANALYSIS AND PREDICTION ON HOUSEHOLD POWER CONSUMPTION

Dr. Tan Yi Fei, Muhammad Naim Bin Abdull Halim, Dr. Guo Xiaoning
Faculty of Engineering, Multimedia University, Cyberjaya, Selangor

Abstract

Electricity is everywhere in this world and is one of the most important resources in our daily lives. A better Energy Management System is paramount for monitoring, analysing and optimising the usage of electricity. In this project, we aim to use data analysis for the prediction on household power consumption utilizing the data collected from electrical smart devices. The data includes nearly 4 years electricity consumption information from 2006 to 2010. Long Short-Term Memory (LSTM) which is an Artificial Recurrent Neural Network (RNN) architecture was chosen as the power prediction model.

Introduction

Big data analytics offers a solution for processing large quantities of data. It is very important to understand the data as discussed in [1] which mostly involved data analysis. For data prediction or forecast ARIMA modelling has been widely used especially in time series data[2]. However, based on experiment conducted[3], it can be observed that LSTM models outperform the ARIMA models.

Method

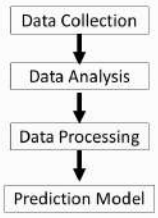

Data Collection:
The dataset used in this work is a publicly available Individual Household Electric Power Consumption Dataset[4]. The electric power consumption is measured with a one-minute sampling rate over a period of nearly 4 years.

Data Analysis:
In this stage, graphical visualization are used to highlight usage patterns in the electric power consumption data. Based on the study and pattern of data, the LSTM prediction model was chosen.

Data Processing:
The data is processed by resampling and restructuring. The purpose of this is to transform the data into the format that can be used by LSTM.

Prediction Model(LSTM):
LSTM is suitable as a prediction model for electric power consumption data due to its capability of learning long-time dependencies. The number of training data is 17,909 and the number of test data is 8,758. The LSTM parameters used are: activation is "ReLU", optimizer is "Adam", one dense layer with 1 unit for the predicted value and epochs are set to 100.

Results and Discussions

The data analysis was initiated by plotting the daily active power consumption. Figure 1 shows an example of daily power usage (on 6 February 2008). The usage is high during certain hours of the day. This may be due to those hours before going work and after work.

Figure 1: Example of single day power Consumption

To further analyse the power usage of the household, the usage of power data was further investigated throughout each year using mean values. Based on Figure 2, it can be seen that the pattern of power consumption over each year is quite similar to each other, there is a drop of power consumption usage from July to September for each year. The usage was high at the beginning and at the end of the year.

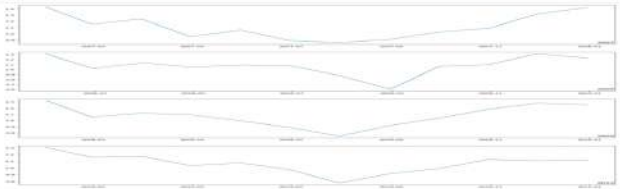

Figure 2: The power consumption by year using mean values

Lastly, the prediction was done by taking 4 continuous power usage data to predict the next power consumption. Figure 3 showed the predicted results follow the actual data closely. Furthermore, the Root Mean Square Error is rather small at 0.605 which means the prediction model was acceptable.

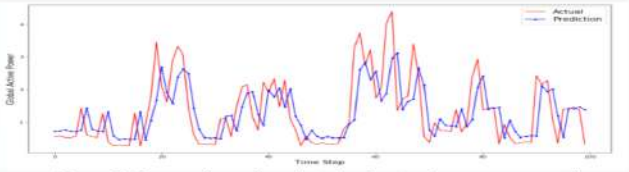

Figure 3: Comparison of predicted and actual power consumption

Conclusion

In this project, a prediction model for power consumption was built. The output of results showed the LSTM prediction model is working well for power consumption data which is in the form of time-series. Currently the model is applied on a publicly available dataset. In the future, the model may be integrated into an Energy Management System to help manage the power usage in a household or an industry.

References

[1] Riahi, Youssra. (2018). Big Data and Big Data Analytics: Concepts, Types and Technologies. 5. 524-528. 10.21276/ijre.2018.5.9.5
[2] Adhikari, R., 2013. An Introductory Study on Time Series Modeling and Forecasting
[3] Siami-Namini, S., & Namin, A.S., 2018. Forecasting Economics and Financial Time Series: ARIMA vs. LSTM. ArXiv, abs/1803.06386
[4] This dataset is made available under the "Creative Commons Attribution 4.0 International (CC BY 4.0)"license.
https://archive.ics.uci.edu/ml/datasets/Individual+household+electric+power+consumption

DESIGN AND IMPLEMENTATION OF AN IOT-ENABLED INTERACTIVE KIOSK

Omar Ayman Mohamed Aboelala, Lee It Ee, Chung Gwo Chin
Faculty of Engineering, Multimedia University

I. Introduction

A smart interactive kiosk system enabled with the internet of things (IoT) technology is proposed and implemented. The proposed interactive kiosk concept can be adopted in smart locker systems for public storages in libraries, museums, universities/colleges, schools, public changing areas and parcel pop boxes.

The system enables the users to select a locker for keeping their belongings in a smart, efficient and secure manner, with minimum credentials such as mobile number and fingerprint. With the aid of Raspberry-Pi and Arduino, the system will register the check-in and check-out times, and then performs a calculation on the storage duration and rental charges. The finger print and RFID accesses are enhanced security features that are introduced to the system.

II. Aims and Objectives

This project aims to implement an **IoT-enabled interactive kiosk system**, which can be adopted in smart locker systems for public storage applications. The main objectives are outlined as follows:

1. To propose the overall layout design of an interactive kiosk.
2. To develop the hardware and software for enabling wireless communication between the kiosk and smartphone.

V. Conclusions

We have implemented a smart IoT-enabled interactive kiosk system, which is highly suited for smart locker systems. The system can be improved with the enhanced feature of checking locker availability and performing pickup/dropoff from mobile devices.

III. Methodology

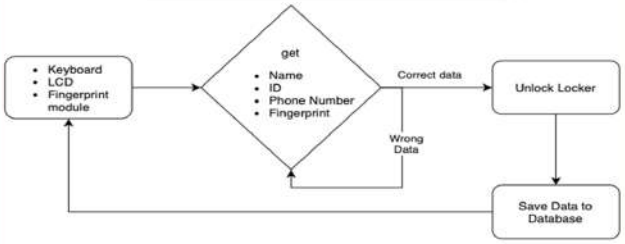

IV. The Smart Locker Prototype

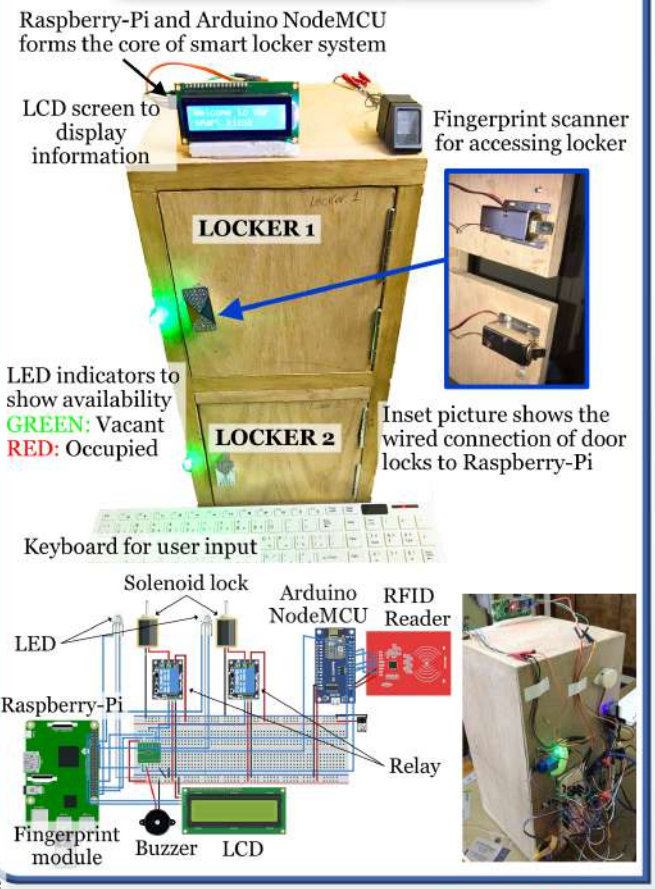

LEFT: Schematic diagram of the proposed system.
RIGHT: Rear view of the prototype with the hardware.

DEVELOPMENT AND PERFORMANCE ANALYSIS ON ANTENNAS FOR 5G COMMUNICATION TECHNOLOGIES

Md. Shabiul Islam*, Md. Mushfiqur Rahman*, Hin Yong Wong*, L. Lee*, Samir Salem Al-Bawri**, Mohammad Tariqul Islam***
*Faculty of Engineering, Multimedia University (MMU), Cyberjaya
**Center for Space Science, Institute of Climate Change, Universiti Kebangsaan Malaysia (UKM), Bangi
***Department of Electrical, Electronic and Systems Engineering , University Kebangsaan Malaysia (UKM), Bangi

Abstract

Several fifth generation (5G) single element antennas in the sub-6 GHz region for terminal edge applications have been presented. The patch antennas are designed with and without metamaterial to reveal the fact that metamaterial has a considerable impact on antenna performance parameters specially in achieving compactness. In addition, a sub-6 GHz multi-layer massive mMIMO base station antenna loaded with metamaterial for 5G applications is also presented. The meta surface is used here to minimize the mutual coupling. This research has invented 360° octa shaped mMIMO antenna with overall 256 elements. Each broadside has 32 elements and capabilities to steer in a wide beam angle with high gain up to 19.5 dBi at 3.5 GHz operating frequency. The antenna is suitable to be combined with RF switch controller and implemented for very precise localization system, a smart antenna system and radar in the future.

Methods and materials

- The main challenge of fifth generation (5G) wireless communications is to enable the end users to experience with applications of high specifications (wide bandwidth and high gain) where the cost should be budget-friendly for the service providers as well as affordable for an individual.
- Metamaterial structure is used to design compact single element antennas for terminal edge applications so that cost can be minimized even when the highly expensive low loss materials, (viz. Rogers 5880 substrate) are used to get wide bandwidth.
- On the other hand, Meta-surface is used in massive mMIMO system to increase the overall network speed and capacity by reducing the co-channel ISI interference as well as the fading effect compared with the current 4G antennas and at the same time by increasing gain.
- Moreover, the system require less power to cover nearly 360° compared to conventional 4G/5G MIMO antennas where additional mechanical parts are needed with the compromise of low gain and undesired multipath interference.

Key features

- Cost effective wide band compact antenna design with low loss materials by using metamaterial structure.
- Multilayer massive mMIMO antenna with a controlled beam direction at azimuth angle.
- High gain and low level of mutual coupling between antenna elements by using meta surface.

Commercial potential

- 5G base station , 5G portable modems, 5G routers, IoT devices and other terminal devices.
- On emergency localization estimation technique.

Special highlights

- One patent is filed for the Octa mMIMO antenna
- 4 publications in ISI indexed journals.
- 3 publications in national and international conferences (already published in IEEE explore)
- 1 gold award in biide exhibition,2019
- 1 silver award in RICES,2019
- 1 best paper award in MJWRT workshop,2019

Discussions

- Metamaterial structures with modified ground results in a compact and wideband antenna.
- Multilayer technique can be used to design massive mMIMO antenna to achieve high gain.
- Superstate made of meta surface can reduce the mutual coupling considerably.

Prototypes and results

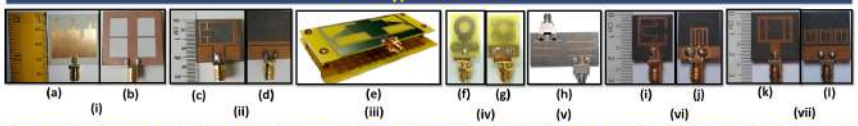

Figure 1: 5G antennas for terminal devices. i) Antenna without metamaterial (a) Front side, (b) Back side. ii) Metamaterial antenna-1, (c) Front side, (d) Back side. iii) Metamaterial antenna-2. (e) with metamaterial superstate . iv) Metamaterial antenna-3, (f) Front side, (g) Back side . v) Metamaterial inspired MIMO antenna-4. vi) Metamaterial antenna-5, (i) Front side, (j) Back side. vi) Metamaterial antenna-6(k) Front side, (l) Back side

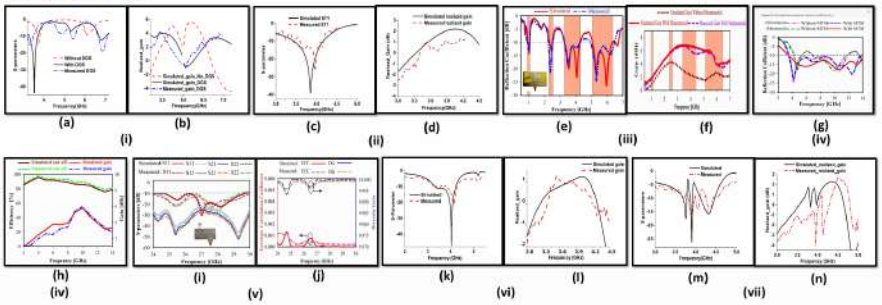

Figure 2: Simulated and measured results of 5G antennas for terminal devices. i) Antenna without metamaterial (a) Reflection coefficient, (b) Realized gain. ii) Metamaterial antenna-1, (c) Reflection coefficient, (d) Realized gain. iii) Metamaterial antenna-2. (e) Reflection coefficient, (f) Realized gain. iv) Metamaterial antenna-3, (g) Reflection coefficient, (h) Realized gain. v) Metamaterial antenna-4, (i) Reflection coefficient, (j) ECC and Realized gain. vi) Metamaterial antenna-5, (g) Reflection coefficient, (h) Realized gain. vii) Metamaterial antenna-6, (g) Reflection coefficient, (h) Realized gain.

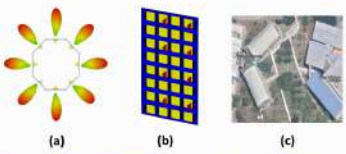

Figure 3: Octa mMIMO Antenna design a) Radiation pattern, b) 32 elements c) MMU implemented area

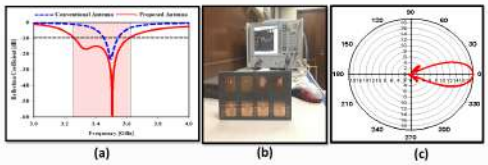

Figure 4: a) Subarray Reflection Coefficient, b) Fabricated 2*4 Subarray antenna d) Radiation pattern.

Conclusions

Several compact wideband antennas are designed, fabricated and the results are validated by the measurement data. A prototype of multilayer mMIMO is fabricated which exhibits high gain with reduced mutual coupling. The state of arts of these projects has a great commercialization potential.

Publications

1. Performance Analysis of a Defected Ground-Structured Antenna Loaded with Stub-Slot for 5G Communication (https://doi.org/10.3390/s19112634)
2. Metamaterial Cell-Based Superstrate towards Bandwidth and Gain Enhancement of Quad-Band CPW-Fed Antenna for Wireless Applications.(https://doi.org/10.3390/s20020457)
3. Compact Ultra-Wideband Monopole Antenna Loaded with Metamaterial.(https://doi.org/10.3390/s20030796)
4. Hexagonal Shaped Near Zero Index (NZI) Metamaterial Based MIMO Antenna for Millimeter-Wave Application. (https://doi.org/10.1109/ACCESS.2020.3028377)

References

[1] (2019, 10/10/2019). 5G Spectrum, GSMA Public Policy Position [Online]. Available: https://www.gsma.com/spectrum/wp-content/uploads/2019/08/spec_5g_positioning_web_07_19.pdf

[2] T. T. Thai, G. R. DeJean, and M. M. Tentzeris, "Design and development of a novel compact soft-surface structure for the front-to-back ratio improvement and size reduction of a microstrip Yagi array antenna," IEEE Antennas and Wireless Propagation Letters, vol. 7, pp. 369-373, 2008.

[3] L. Huitema and T. Monédière, "Compact antennas—An overview," in Progress in Compact Antennas: IntechOpen, 2014.

[4] N. Rajak and N. Chattoraj, "A bandwidth enhanced metasurface antenna for wireless applications," Microwave and Optical Technology Letters, vol. 59, no. 10, pp. 2575-2580, 2017.

[5] M. Alibakhshikenari, M. Khalily, B. S. Virdee, C. H. See, R. A. Abd-Alhameed, and E. Limiti, "Mutual coupling suppression between two closely placed microstrip patches using EM-bandgap metamaterial fractal loading," IEEE Access, vol. 7, pp. 23606-23614, 2019.

[6] R. Mark, N. Rajak, K. Mandal, and S. Das, "Metamaterial based superstrate towards the isolation and gain enhancement of MIMO antenna for WLAN application," AEU-International Journal of Electronics and Communications, vol. 100, pp. 144-152, 2019.

[7] L. Si, H. Jiang, X. Lv, and J. Ding, "Broadband extremely close-spaced 5G MIMO antenna with mutual coupling reduction using metamaterial-inspired superstrate," Optics express, vol. 27, no. 3, pp. 3472-3482, 2019.

Acknowledgement

- This work was supported by Faculty of Engineering, Multimedia University, Cyberjaya, Malaysia under research grant MMUE/180010, TM R&D.
- Special thanks to CWT laboratory of MMU to support the work
- Special thanks to Radio & Satellite Laboratory, Microwave laboratory and Near Field Laboratory to fabricate the prototypes

Emotion Recognition for Mental Health Monitoring System

Nor Azlina Binti Ab. Aziz[a], Md Armanur Rahman[a], Chy Mohammed Tawsif Khan[a], Sharifah Noor Masidayu Binti Sayed Ismail[b], Nor Hidayati Abdul Aziz[a], Nor Hidayah Mohamad[a], Syabeela Syahali[a], Rosli Besar[a], Siti Zainab Ibrahim[b], Kamarulzaman Ab Aziz[c]
[a]Faculty of Engineering & Technology, [b]Faculty of Information Science & Technology, [c]Faculty of Management,
Multimedia University

Introduction

Emotion recognition system identifies human emotion like happiness, sadness, anger, disgust and fear. These emotions can be detected via various modalities such as facial expression analysis, voice intonation, and physiological signals like the brain's electroencephalogram (EEG) and heart's electrocardiogram (ECG). The emotion recognition system allows machines to recognize human emotions and react to it.

Emotion Recognition & Mental Health

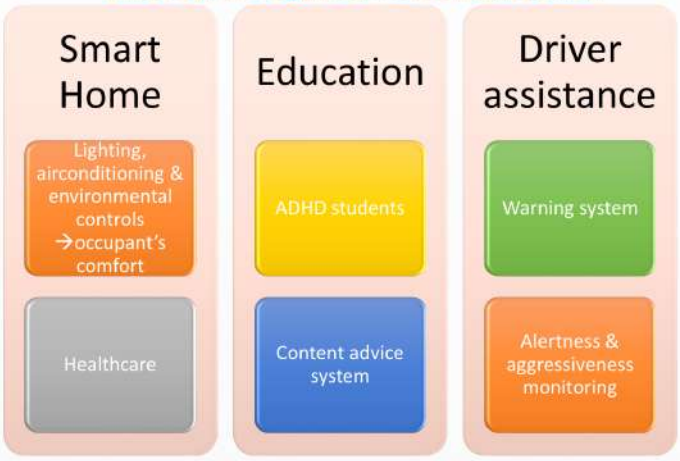

Knowledge Transfer Program

The KTP was conducted at Universiti Tun Hussein Onn (UTHM) in Feb 2020, with participation of 177 students from Faculty of Electrical & Electronics Engineering.

Methodology & Results

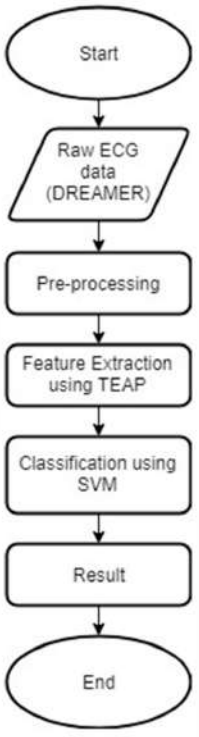

Feature	Description
IBI (inter beat interval)	Mean IBI, HRV (standard deviation (IBI))
MSE (mean square error)	Multiscale entropy at 5 levels [30]
Tachogram Power	log (log (log (log (log (log (where LF:f ∈ [0.01, 0.08]Hz, MF:]0.08, 0.15]Hz, and HF:]0.15, 0.4]Hz
PSD (power spectral density)	Log($P_X(f)$), f ∈ ([0, 0.01],[0.1,0.2],[0.2,0.3],[0.3,0.4]}Hz log (where LF:f ∈ [0.0,0.08]Hz & HF:f ∈ [0.15, 5.0]Hz

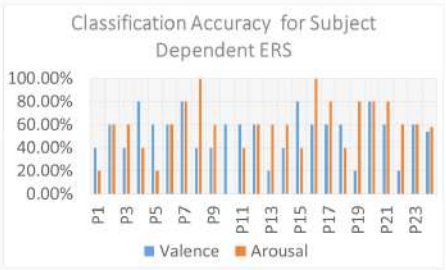

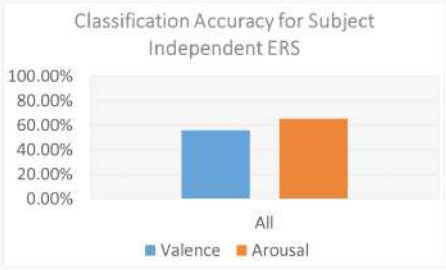

The findings show that subject independent emotion recognition system achieves better classification accuracy for both arousal (65.4% vs 58.3%) and valence (55.8% vs 53.9%) in comparison to the average of classification accuracy found by the subject dependent system.

Acknowledgement

This project is funded by Fisabilillah R&D Grant Scheme from Tabung Amanah Zakat Multimedia University (FRDGS2018/11).

ENERGY HARVESTER USING PIEZOELECTRIC TRANSDUCER

Dr. Sin Yew Keong and Mr. Wassem Ibrahim
Faculty of Engineering, Multimedia University, Persiaran Multimedia, 63100 Cyberjaya, Selangor

Project Background

Electrical energy is a basic need in the modern life and its demand is increasing. Recently, the most common sources used to generate electrical energy are coal, natural gas and petroleum. Unfortunately, these sources are non-renewable. Hence, electrical energy harvested from renewable sources is developed rapidly nowadays. In the past 25 years, researchers have the interest in converting mechanical energy from human motion into electrical energy. This energy harvesting produces a very small amount of power that can be used in recharging batteries of low-energy electronic devices [1]. Piezoelectricity is the electricity generated from mechanical pressure. Positive and negative charges are distributed evenly when no mechanical stress is applied on the piezoelectric material. However, deformation of lattice structure due to the applied mechanical stress over piezoelectric material will generate electric potential [2]. Lead zirconate titanate (PZT) is the commonly used material in piezoelectric. However, PZT is hazardous because it contains >60% lead by weight. Barium titanate is a lead free piezoelectric material which is developed in 1940s and 1950s. Barium titanate does not have very high piezoelectric constant but it has high permittivity [3].

Results & Discussions

In this project, the energy harvester was designed by placing the 5 piezoelectric transducers under a 14 cm × 14 cm acrylic plate. These piezoelectric transducers were either connected in parallel or series connection for system testing. The output voltages generated by piezoelectric transducers in parallel and series connections with different human weights were compared. Three different human weights were applied, 78 kg, 92 kg and 115 kg, respectively. When the acrylic plate was stepped, mechanical stress was applied to piezoelectric transducers due to human weights. The mechanical stress changed electrical polarisation of piezoelectric transducers and random output voltages were generated. From the results, piezoelectric transducers connected in parallel always generate higher output voltages compare to piezoelectric transducer in series connection. Based on 115kg human weight results, piezoelectric transducers connected in parallel generated 69.6 mV, but generated 55 mV with series connection. According to the graph of output voltages by piezoelectric transducers in parallel connection, 30 mV is predicted to be generated by 70 kg human weight. 100 steps are required to generate 3 V. As a result, 400 steps from a 70 kg human can fully charge a 12 V rechargeable battery.

Series Connection

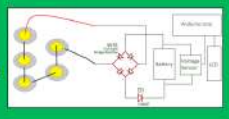

Series Connection (5 sensors)

Weight	Steps					Average
	S1	S2	S3	S4	S5	
78kg	32mV	23mV	27mV	32mV	38mV	30.4mV
92kg	51mV	49mV	45mV	55mV	43mV	47.8mV
115kg	60mV	57mV	51mV	54mV	53mV	55mV

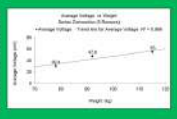

Parallel Connection

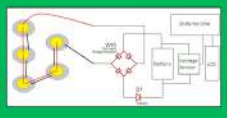

Parallel Connection (5 sensors)

Weight	Steps					Average
	S1	S2	S3	S4	S5	
78kg	39mV	32mV	41mV	32mV	38mV	36.4mV
92kg	59mV	53mV	45mV	51mV	43mV	50.2mV
115kg	70mV	66mV	73mV	62mV	68mV	69.6mV

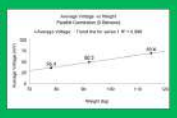

Methods & Materials

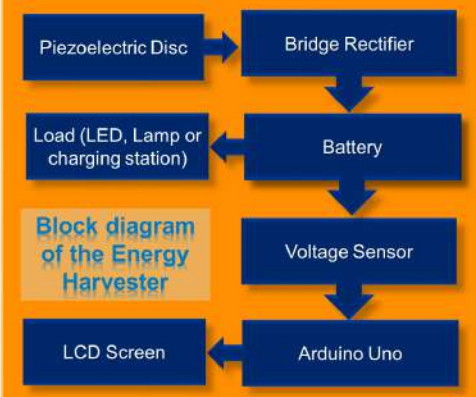

Block diagram of the Energy Harvester

Testing on Energy Harvester

Conclusions

In this project, an energy harvester to generate voltages from human steps is successfully fabricated. The concept of energy harvester has a great potential. For example, it can be inserted in shoe insoles to work as power source to charge portable power bank. It also can be installed at the entrance of shopping malls and light railway stations where foot traffic is high. However, further researches on the converting circuit and storing mechanism are required to achieve higher conversion rate and storing capacity of energy harvester.

References

1. M. A. Adhithan, K. Vignesh, and M. Manikandan, "Proposed Method of Foot Step Power Generation Using Piezo Electric Sensor," Int. Adv. Res. J. Sci. Eng. Technol., vol. 2(4), pg 25-28, 2015.
2. A. Dakhole and A. Boke, "Electrical Energy Harvesting from Mechanical Pressure of Vehicles Using Piezoelectric Generators," IOSR J. of E&E Eng., vol.12(2), pg 46-49, 2017.
3. E. Aksel and J. L. Jones, "Advances in Lead-Free Piezoelectric Materials for Sensors and Actuators", Sensors, vol. 10, pg 1935-1954, 2010.

ENERGY SUPPLY & SUSTAINABILITY IN RURAL AREAS

Dr. Palanichamy Naveen
Faculty of Computing and Informatics
Multimedia University

Dr. Goh Vik Tor
Faculty of Engineering
Multimedia University

Jayanthi Nishanth
Faculty of Engineering
Multimedia University

Introduction

The adoption of the Industrial Revolution 4.0 is carried out across various sectors, and the energy sector is not an exception. The power infrastructure requires an intelligent and real-time system with bilateral communication and control facilities is known as the Smart Grid[1].

For the successful functioning of smart grid, advanced measuring units, such as the Phasor Measurement Units (PMUs), are needed. PMUs are used as the backbone to sense and measure system parameters and its data are utilized to improve the interface and decision support.

The optimal placement of PMUs is important to:

- obtain full observability of the grid with a minimum number of PMUs installed
- prepare for combinations of contingency events, prevent wide-area blackouts and fast recovery from an emergency state

The various techniques [2-10] to solve the PMU placement problem requires vast computation time and increases the cost of decision making. In this research, we proposed a cloud-based algorithm for optimal PMU placement, which ensures complete observability of the smart grid. The efficacy of the proposed algorithm was validated through the IEEE test systems.

Methodology

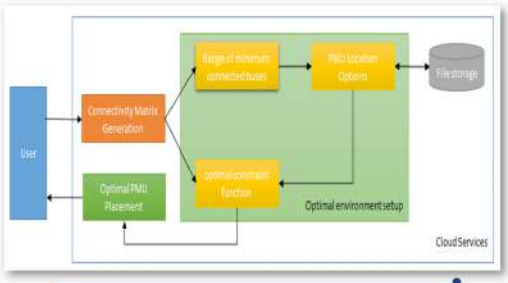

Proposed Algorithm

Example: A nine bus system (Fig . Courtesy – Naveen, SST Journal Sep.2020)

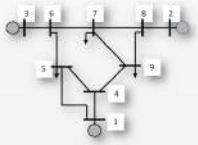

1. Connectivity Matrix Generation

$$A_{i,j} = \begin{cases} 1, & i = j \\ 1, & i \text{ and } j \text{ are connected} \\ 0, & \text{otherwise} \end{cases}$$

$$A = \begin{bmatrix} 1&0&0&1&1&0&0&0&0 \\ 0&1&0&0&0&0&0&1&0 \\ 0&0&1&0&0&1&0&0&0 \\ 1&0&0&1&1&0&0&0&1 \\ 1&0&0&1&1&1&0&0&0 \\ 0&0&1&0&1&1&1&0&0 \\ 0&0&0&0&0&1&1&1&1 \\ 0&1&0&0&0&0&1&1&1 \\ 0&0&1&0&0&1&1&1&1 \end{bmatrix}$$

2. PMU Location Options

$$Finite\ matrix = \begin{bmatrix} Rows\ with\ two\ Ones \\ \vdots \\ Rows\ with\ three\ Ones \\ \vdots \\ Rows\ with\ four\ ones \\ \vdots \\ Rows\ with\ n\ ones \end{bmatrix}$$

3. Optimal Constraint function

Finite Matrix → Connectivity matrix ≥ 1

$$\begin{bmatrix} Rows\ with\ two\ Ones \\ \vdots \\ Rows\ with\ three\ Ones \\ \vdots \\ Rows\ with\ four\ ones \\ \vdots \\ Rows\ with\ n\ ones \end{bmatrix} \rightarrow \begin{bmatrix} 1&0&0&1&1&0&0&0&0 \\ 0&1&0&0&0&0&0&1&0 \\ 0&0&1&0&0&1&0&0&0 \\ 1&0&0&1&1&0&0&0&1 \\ 1&0&0&1&1&1&0&0&0 \\ 0&0&1&0&1&1&1&0&0 \\ 0&0&0&0&0&1&1&1&1 \\ 0&1&0&0&0&0&1&1&1 \\ 0&0&1&0&0&1&1&1&1 \end{bmatrix} \geq 1$$

4. Optimal solution is the minimum PMUs for full observability of the system.

Bus No	1	2	3	4	5	6	7	8	9
PMU Location	0	0	0	0	1	1	0	1	0

Results and Discussion

- **98.87% reduction** in the number of rows results in a considerable reduction in the computational time, i.e., 5.6%.
- The **proposed approach is much faster** than the conventional Invasive Weed Optimization (IWO) algorithm.

IEEE 14 Bus

PMU Placed	IWO	Proposed algorithm
Finite matrix rows	16384	6461
PMU placement	Buses 2, 6, 7 and 9	Buses 2, 6, 7 and 9
Observability	19	19
Time (ms)	177	177

IEEE 24 Bus

PMU Placed	IWO	Proposed algorithm
Finite matrix rows	16777216	190026
PMU placement	Buses 2, 3, 8, 10, 16, 21, and 23	Buses 2, 3, 8, 10, 16, 21, and 23
Time (ms)	256913.40	242503.57

Conclusion

The suggested cloud-based optimal PMU placement strategy presented the concept of optimal PMU placement.

Proposed cloud-based optimal PMU placement strategy is able:

- To provide optimal PMU placement locations with full system observability
- To reduce the cost and computation time

The efficacy of the suggested algorithm was proved through two IEEE test systems.

Others

Acknowledgement
The authors gratefully acknowledge MMU, Cyberjaya, for the mini fund (2019-20) provided for successfully carrying out this research.

References

1. *SURUHANJAYA TENAGA (ENERGY COMMISSION), "Towards a World-Class Energy Sector Energy Malaysia", in Energy Malaysia. 2018, The IBR Asia Group Sdn. Bhd.*
2. *D. Rasa Prabha, T. Jayabarathi, Optimal placement and sizing of multiple distributed generating units in distribution networks by invasive weed optimization algorithm, Ain Shams Engineering Journal, 7, 683–694, 2016.*
3. *Miller, Heloisa H., and Carlos A. Castro. "Genetic algorithm-based phasor measurement unit placement method considering observability and security criteria." IET Generation, Transmission & Distribution 10.1 (2016): 270-280.*
4. *Matsukawa, Yoshiaki, et al. "Reliably Optimal PMU Placement using Disparity Evolution-based Genetic Algorithm." PERTANIKA JOURNAL OF SCIENCE AND TECHNOLOGY25 (2017): 103-110.*
5. *Bikash, Arvind, and H. D. Mathur. "Identification of optimal locations of PMUs for WAMPAC in smart grid environment." Advancements in Power and Energy (TAP Energy), 2015 International Conference on. IEEE, 2015.*
6. *Xie, Ning, et al. "A graph theory based methodology for optimal PMUs placement and multiarea power system state estimation." Electric Power Systems Research 119 (2015): 25-33.*
7. *Khorram, Ebrahim, and Mehdi Taleshian Jelodar. "PMU placement considering various arrangements of lines connections at complex buses." International Journal of Electrical Power & Energy Systems 94 (2018): 97-103.*
8. *Kim, Taedong, and Stephen J. Wright. "PMU placement for line outage identification via multinomial logistic regression." IEEE Transactions on Smart Grid 9.1 (2018): 122-131.*
9. *Ahmadi, A., Y. Alinejad-Beromi, and M. Moradi. "Optimal PMU placement for power system observability using binary particle swarm optimization and considering measurement redundancy." Expert Systems with Applications 38.6 (2011): 7263-7269.*
10. *Nazari-Heris, M., and B. Mohammadi-Ivatloo. "Application of heuristic algorithms to optimal PMU placement in electric power systems: An updated review." Renewable and Sustainable Energy Reviews 50 (2015): 214-228.*

Life Made Easier™ | TM Group

Energy-Efficient Interference Management Techniques for Multi-cell Multi-tier HetNets

Project Leader: Dr. Ng Yin Hoe
Member: Dr. Tan Chee Keong
Graduate Research Assistant: Shornalatha Euttamarajah
Funding: Multimedia University Graduate Research Assistant Scheme
Duration: 1 February 2018 – 31 January 2021

Problem Statement

In recent years, energy harvesting has emerged as a promising solution to address the increased energy consumption issue in 5G heterogeneous networks (HetNets). However, due to the geographical heterogeneity of harvesting renewable energy and inhomogeneous distribution of users in HetNets, the energy harvested by base stations may not fit their load conditions and hence may lead to low energy efficiency (EE). In this project, hybrid-powered coordinated multi-point **(CoMP)** joint processing based HetNets are considered. To improve the EE of such a system, it is necessary to jointly design the transmit power allocation (PA), energy cooperation, user-association and base station on-off switching.

Objectives

1. To propose an energy-efficient joint transmit PA and energy cooperation technique for the downlink of hybrid-powered CoMP-enabled HetNets.
2. To incorporate user-association and base station on/off switching to the proposed technique.
3. To improve the performance of the proposed technique under imperfect channel state information conditions.

Contributions

A novel joint transmit PA and energy cooperation technique is proposed using a combinatorial optimization algorithm. The benefits of the proposed techniques are:
1. Higher energy efficiency. 2.Reduction in grid power consumption.

Results

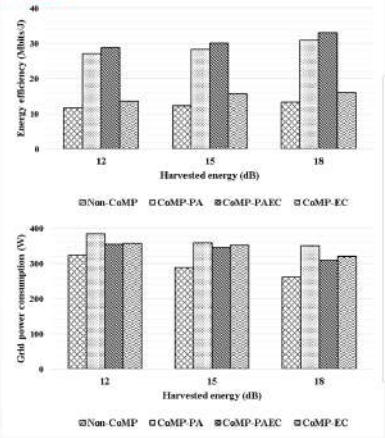

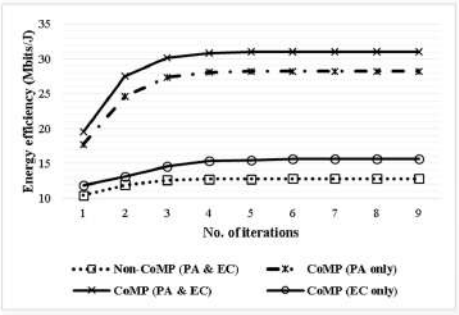

System Model

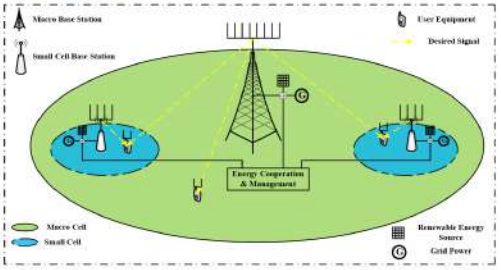

Methodology

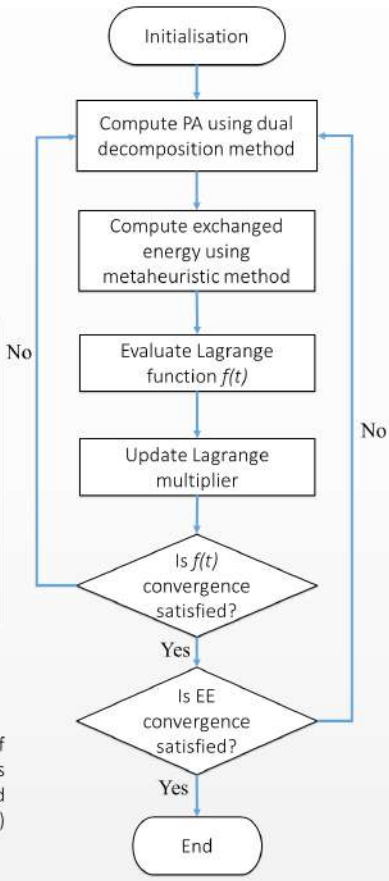

Conclusion

Both the data and energy cooperation are proven to play a significant role in improving the EE of the communication system. The system with data cooperation (CoMP) performs nearly 2.5 times better than the system without data cooperation (Non-CoMP). On the other hand, joint data and transmit power allocation (CoMP-PA) contributes to better EE (nearly double the amount) compared to the system without efficient power allocation (CoMP-EC).

Publications – Journal Papers

The techniques proposed have been published in the following journals:

Euttamarajah, S., Ng, Y. H., & Tan, C. K. (2020). Energy-Efficient Joint Power Allocation and Energy Cooperation for Hybrid-Powered Comp-Enabled HetNet. IEEE Access, 8, 29169-29175.

Energy-Efficient Resource Allocation with Interference Mitigation for Cognitive Heterogeneous Cloud Radio Access Network (CH-CRAN)

Project Leader: Dr. Ng Yin Hoe
Member: Dr. Tan Chee Keong
Graduate Research Assistant: Prabha Kumaresan
Funding: Multimedia University Graduate Research Assistant Scheme
Duration: 1 Jun 2017 – 31 May 2020

Problem Statement

In recent years, non-orthogonal multiple access (NOMA) has emerged as one of the promising radio access techniques for 5G systems. In the existing user clustering techniques, the number of users for each of the clusters formed is fixed. This results in poor throughput performance as the channel heterogeneity and diversity are not fully exploited.

Objectives

1. To determine the optimum user clustering for throughput maximization in the downlink of 5G NOMA systems.
2. To design improved user clustering methods that maximize the throughput performance of the 5G NOMA systems.
3. To evaluate the performance of the proposed and existing user clustering methods in various 5G NOMA deployment scenarios.

Contributions

Three novel adaptive user clustering (AUC) techniques have been devised. Specifically, a B-FS strategy is proposed to find the optimum user clustering. However, the computational complexity of this scheme is prohibitively high. To address this issue, another two AUC schemes that leverage on PSO and ANN are developed to attain near-optimal throughput performance at a moderate complexity.

Publications – Journal Papers

The techniques proposed have been published in the following journals:

1. S. P. Kumaresan, C. K. Tan, and Y. H. Ng, "Efficient User Clustering Using a Low-Complexity Artificial Neural Network (ANN) for 5G NOMA Systems", IEEE Access, vol. 8, pp. 179307 - 179316, Sep 2020.
2. S. P. Kumaresan, C. K. Tan, C. K. Lee, and Y. H. Ng, "Adaptive User Clustering for Downlink Non-Orthogonal Multiple Access (NOMA) based 5G Systems Using Brute Force Search", vol. 31, ETT, Aug. 2020.
3. S. P. Kumaresan, C. K. Tan, C. K. Lee, and Y. H. Ng, "Low-Complexity Particle Swarm Optimization based Adaptive User Clustering for Downlink Non-Orthogonal Multiple Access deployed for 5G Systems", WRSTSD, in press.

Results

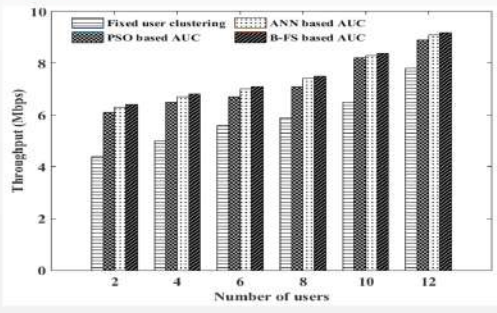

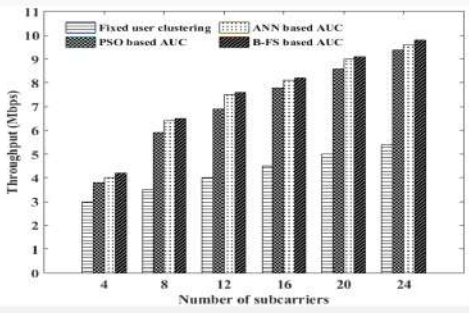

Proposed ANN-based adaptive user clustering technique

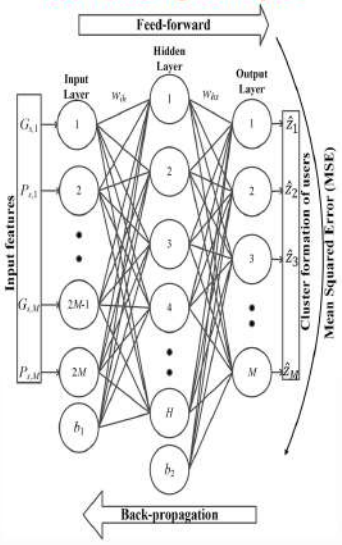

Proposed PSO-based adaptive user clustering technique

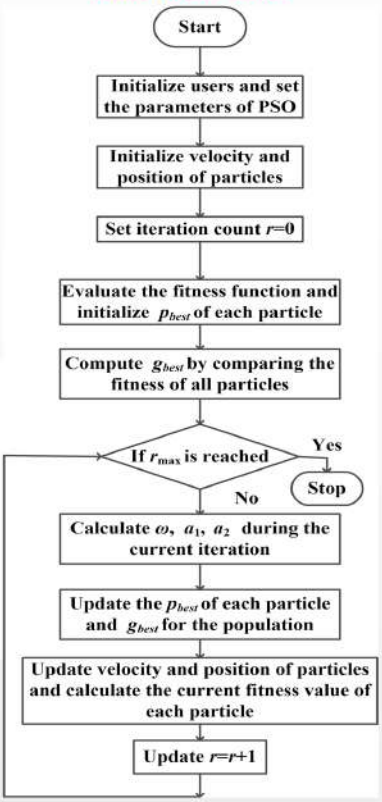

FPGA IMPLEMENTATION OF OFDM TRANSCEIVER FOR MM WAVE COMMUNICATION SYSTEM (5G)

Dr. Nor Hidayati Abdul Aziz, Dr. Lim Heng Siong, Dr. Thangavel Bhuvaneswari
Faculty of Engineering & Technology
Melaka, Malaysia.
hidayati.aziz@mmu.edu.my

Introduction: Orthogonal Frequency Division Multiplexing (OFDM) is a promising modulation technique because of its ability to handle multipath frequency selective channels with a simple receiver. The objective of this project is to design and implement a baseband OFDM transmitter and receiver on FPGA hardware.

In this project, we report experimental results on the performance of the physical layer of filter bank multicarrier with off-set quadrature amplitude modulation (FBMC/OQAM) system as measured in a testbed implemented with FPGA (field-programmable gate array). A physical layer approach which is compatible with the IEEE 802.11a standard has been developed and tested for timing synchronization, carrier frequency offset (CFO) correction, channel estimation, equalization and residual phase error compensation. Due to the inherent intrinsic imaginary interference in FBMC/OQAM, a specially designed pilot scheme has been used to deal with the residual phase error. Three-phase noise estimation schemes such as phase noise compensation (PNC) method, extended Kalman filter (EKF) and modified blind phase searching (MBPS) method have been evaluated. To further suppress the residual interference and phase error, an iterative soft decision feedback (ISDF) technique can be employed after channel equalization. The performance of the proposed system has been evaluated via experiments and simulations for indoor environment.

Methodology: The structure of the FBMC/OQAM frame is designed to be similar to IEEE 802.11a standard that is used in WARP kit for 64-subcarrier OFDM system; only the pilot and data subcarrier locations are changed.

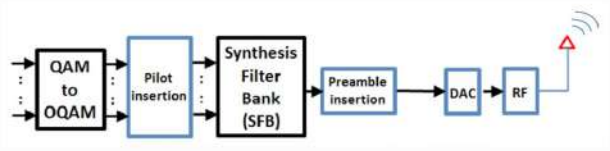

Figure 1: FBMC/OQAM transmitter implemented in WARP kit

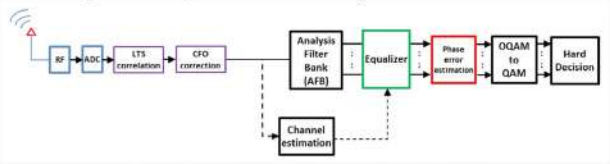

Figure 2: FBMC/OQAM receiver implemented in WARP kit

Experimental setup: The evaluation of the proposed FBMC/OQAM system is performed using two WARP v3 kits operating at 2.412 GHz, connected through a gigabit Ethernet switch to a personal computer (PC). MATLAB is used for constructing the transmitted FBMC/OQAM signal and performing the signal processing techniques for the received signal.

The field measurements have been carried out along the corridor on the second floor of Faculty of Engineering and Technology, Multimedia University. The transmitter (TX) board is placed at the height of 1.6m, at the location denoted by the solid square in Fig. 3. The receiver (RX) board is placed at the height of 0.75m, and moved along the straight dashed line.

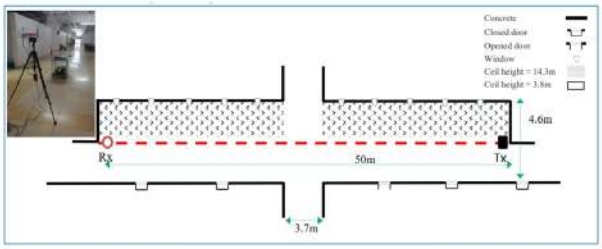

Figure 3: Corridor layout of the experimental setup

Results: The performance of different techniques to eliminate the phase error have been tested. Two indoor channel models (B & C) are simulated for a typical residential home and small office.

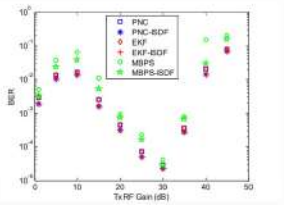

Figure 4a: BER vs Tx RF gain of FPGA board

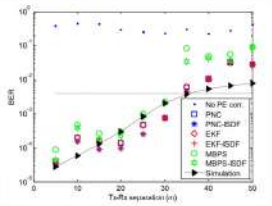

Figure 4b: BER vs Tx-Rx separation

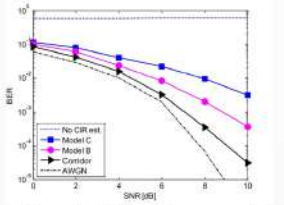

Figure 5a: BER performance of FBMC/OQAM system

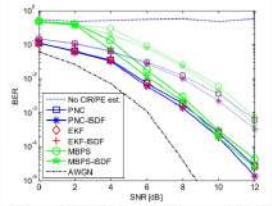

Figure 5b: BER vs SNR in model B (solid line) and model C (dashed line)

Discussion & Conclusion: Low complexity methods to compensate for phase noise have been evaluated via experiments and numerical simulations. In particular, the MBPS method is optimized to realize a good trade-off between computational complexity and performance. Moreover, the pilot power is optimized for efficient phase estimation in PNC and EKF methods. It is found that MBPS method performs fairly well at low phase noise and high SNR, however, at high phase noise and low SNR, the PNC and EKF can tolerate a much larger phase noise than MBPS method. In the presence of severe multipath fading, the IMI become significant. Thus ISDF technique can be used to eliminate the residual interference and enhance the system performance. It is worth mentioning that the PNC provides a better choice than other methods with a good trade-off between complexity and performance.

Acknowledgment: This research is supported by MMU minifund MMUI/190016.

FUZZY LOGIC MODELLING OF 3D PRINTED ALUMINIUM PART

Wee Zhen Xun, Dr. Chockalingam Palanisamy

Introduction

The manufacturing sector is developing new and improved methods in their manufacturing processes which leads to 3D printing technology. However, the final quality of the 3D printed specimen is difficult to be determined but it is crucial for the mass production in the manufacturing sector. The objective of the study is to develop a Fuzzy Logic Modelling in predicting the final quality of a 3D printed aluminium part from different set of input parameters.

Methods & Materials

The study is conducted using the Design of Experiment (DOE) approach with Central Composite Design (CCD) illustrated in Figure 1 with a set of control input parameters shown in Table1. The 15 sets of Aluminium-Polylactic Acid (Al-PLA) specimen are printed using MakerBot Replicator 5th Generation 3D Printer according to the Design Matrix Table as shown in Table 2. Mechanical testing specimen used in the project are tensile testing, compression testing and hardness testing. Using the data from mechanical testing, the Fuzzy Logic Model of AL-PLA presented in Figure 2 is developed using the Fuzzy toolbox from MATLAB software with 3 inputs and 3 outputs parameters with 15 sets of fuzzy rules.

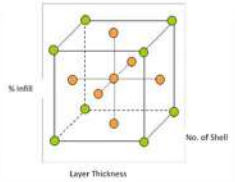

Figure 1 Central Composite Design

Table 1 Input Parameters

Parameter	Levels		
Level Code	-1	0	1
Layer Thickness	0.1 mm	0.2 mm	0.3 mm
Number of shells	1	2	4
Infill Density	20%	40%	80%

Table 2 Design Matrix Table

No.	Coded values			Actual values		
	Layer Thickness	No. of Shells	Infill Density	Layer Thickness, mm	No. of Shells	Infill Density, %
1	-1	-1	-1	0.1	1	20
2	1	-1	-1	0.3	1	20
3	-1	1	-1	0.1	4	20
4	1	1	-1	0.3	4	20
5	-1	-1	1	0.1	1	80
6	1	-1	1	0.3	1	80
7	-1	1	1	0.1	4	80
8	1	1	1	0.3	4	80
9	-1	0	0	0.1	2	40
10	1	0	0	0.3	2	40
11	0	-1	0	0.2	1	40
12	0	1	0	0.2	4	40
13	0	0	-1	0.2	2	20
14	0	0	1	0.2	2	80
15	0	0	0	0.2	2	40

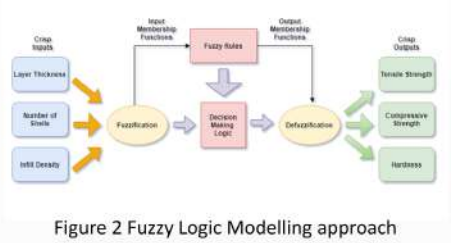

Figure 2 Fuzzy Logic Modelling approach

Results & Discussions

The results obtained from the mechanical testing are tabulated and analyzed in the form of bar charts as shown in Figures 3(a),(b) and (c). With the mechanical test data, Fuzzy Logic Modelling of Al-PLA is developed with 3 inputs and 5 outputs membership functions along with 15 sets of fuzzy rules. The Fuzzy Rules Viewer from the Fuzzy toolbox in MATLAB software is used to predict the output for 5 different combinations of input parameters. Then, with the combination of input parameters, 5 specimens are printed and tested for mechanical properties are shown in Table 3 to validate the performance of developed model. Comparing the results of fuzzy model predicted data and mechanical testing data, the percentage variation is less than 5%, proved that developed Fuzzy Logic Model is valid.

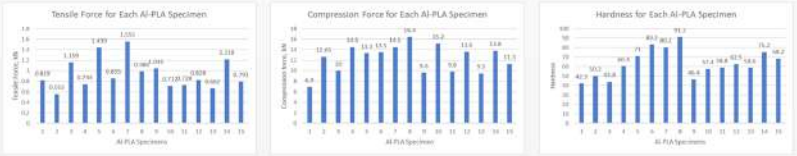

Figure 3(a) Tensile Test Results, (b) Compression Test Results, (c) Hardness Test Results

Table 3 Validation Experiment Results

Conclusion

The objective of this study is to develop a Fuzzy Logic model to predict the mechanical strength of 3D-printed Al-PLA. The model is developed in MATLAB to evaluate its performance. The developed model has less than 5% variations from experimentally collected data. This proves that developed model is valid and the objective is successfully achieved.

msu management & science university | RICES2020

IOT TOWARDS SMART MONITORING AND CONTROL OF HYBRID-SYSTEM FOR STANDALONE ELECTRICITY GENERATION

Assoc. Prof. Dr. Mohammed N. Abdulrazaq
Umira Najwa Binti Saiman
Management & Science University (MSU)
(RIPHEN)

Problem Statements

- Numerous rural areas in Malaysia face difficulties reaching the electrical grid connection systems. Communities situated on terrains with small water resources such as rainwater, small rivers, and springs rarely have a single-day period with no direct sunlight.
- Natural resources such as rainwater and sunlight are affordable but unfortunately not exploited correctly.
- Independent use of a single energy source in the off-grid application usually leads to a considerably oversized generation and storage system, which causes a higher operating and lifestyle cost.

Objectives

- To implement standalone renewable hybrid(hydro-solar) energy power generation system using IoT.
- To utilize IoT approach in hybrid (hydro-solar) system for monitoring and control irrigation system.
- To monitor and control real-time interactive electrical power systems.

Novelty and Inventiveness

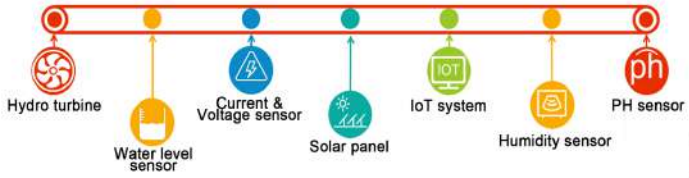

Impact to the society

This project will be highly beneficial, especially to indigenous people (orang asli) and farmers as farming accounts for more than 60% of the occupation in our country. Crop production will be increased if our system is used as it uses IoT and different sensors to gather information regarding irrigation outputs and also provides protection to farms. Also, they can use remote technology to activate/deactivate water pumps which are powered by clean sources of energy thus keeping the environment clean.

Project Development

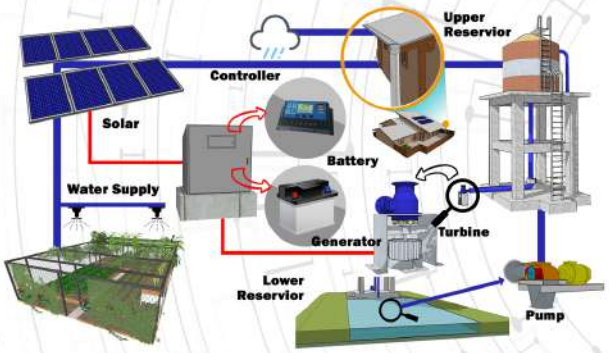

Market Potential & Commercialization

- Rural Areas
- Renewable Energy
- Environmental
- Agricultural

SUSTAINABLE DEVELOPMENT GOALS

JOMSOLAT: A PRAYER ADHERENCE SYSTEM

Dr. Sarina Mansor, Assoc. Prof. Ir. Dr. Hezerul Abdul Karim
Dr. Ooi Chee Pun, Dr. Tan Wooi Haw
Liew Xuan Wei, Ahmad Syamim Mustaqim, Ibrahim AlKhalifah
Faculty of Engineering, Multimedia University, Cyberjaya

INTRODUCTION

Solat is very important in Islam, which is the first pillar in the faith of Islam. It is an obligatory religious duty for every Muslim.

Most Islamic Apps are mainly focused on Azan reminder, Qibla direction, Quran companion and Solat interactive videos [1],[2]. To the best of our knowledge, no existing application or system that is able to monitor and record daily Solat activities.

This research aims to develop a smart prayer adherence system using the Internet-of-Things (IoT) platform, which is able to monitor, remind and assist daily prayers for young children and elderly Muslim.

METHODOLOGY

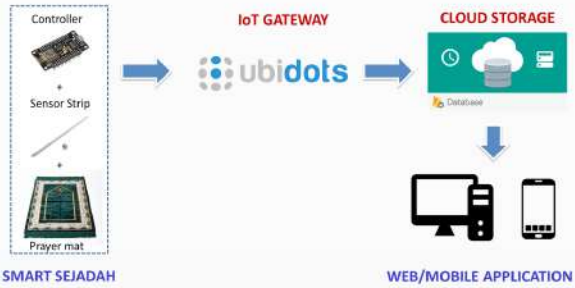

The designed Prayer Adherence System consists of two main parts:

- **'Smart Sejadah'**: A prayer mat is embedded with electronic components (sensor and controller) [3], which will record the Solat activities and send the information to the server.

- **Web/Mobile application**: A web/mobile application is developed to display the Solat activities based on the information stored in the server.

The Smart Sejadah and the Web Application are integrated using IoT platform.

ACKNOWLEDGEMENT

This project is funded by FISABILILLAH R&D GRANT SCHEME (FRDGS)

DESIGNED SYSTEMS

Design 1: A Prayer Adherence System for Muslim Children

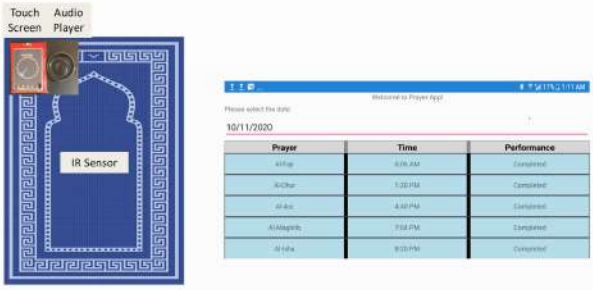

Design 2: A Prayer Adherence System for Elderly Muslims

CONCLUSIONS

With the advancement of Internet techologies, it is feasible to build a low-cost smart prayer adherence system.

Design 1 will be useful for parents (especially working parents) to keep track of their children daily prayers. Design 2 will be useful to monitor and assist prayer activities of elderly Muslims with cognitive impairment.

This research is parallel to the National Industry 4.0 Policy Framework that encourages IoT incorporation in daily life.

REFERENCES

[1] The 21 Most Innovative Global Muslim Apps of 2017 (2017): [online] Available at: https://ummahwide.com/the-21-most-innovative-global-muslim-apps-of-2017

[2] Muslim Kids Guide and Salah (2018): [online] Available at: https://play.google.com/store/apps/details?id=com.salah.osratouna

[3] Kasman and V.G Moshnyaga, "A Smart Mat for Assisting Muslims in Praying", ICCE, 2017.

LATEX GLOVE CUTTING AND BINDING MECHANISM WITH COMPUTERIZED PROTEIN ESTIMATION SYSTEM

Prof. Ir. Dr. Sim Kok Swee, Low Lay Chen, Toa Chean Khim, Tan Jin Long, Eng Yun Hao, Lim Zheng You

Introduction

Health care workers and industry workers with frequent contact with latex gloves are at risk for latex allergy. To prevent latex sensitization, skin allergy reactions, and associated risk factors, the protein concentration level of the glove must be controlled. A newly computerised protein concentration detection has been introduced to enhance the sampling efficiency through an automated chemical binding system followed by digital image acquisition, image processing, and data analysis. Overall, this project is able to reduce the detection time to 1 hour as compared to conventional methods which require at least 5 hours to complete the process of protein concentration detection.

Figure 1: Workers Expose to Latex Allergy

Methods & Materials

The proposed system comprises of 4 processes which include: Glove Stamping, Automated Chemical Binding, Digital Colour Image Acquisition and Image Processing & Data analysis.

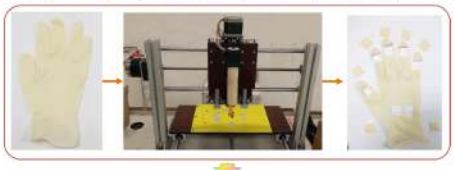

Glove Cutting
Cut latex glove into 7 pieces of Raw sample.

Chemical Binding
Perform chemical test automatically on Raw sample to obtain Chemical-Binded sample.

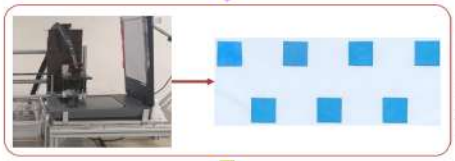

Digital Colour Image Acquisition
Convert Chemical-Binded sample into digital image using Flatbed scanner.

Image Processing & Data Analysis
Calculate colour difference on all 7 pieces of sample and predict the protein concentration based on the ΔE value.

Figure 2: Procedure of the Computerised Protein Concentration Detection

Uniqueness

- ❑ Fast: The protein concentration detection process of the proposed computerised method is faster than conventional methods.
- ❑ Simple: Easier to use system equipped with Unique Remote Control Stamping machine and Automated Chemical Binding machine. The GUI handles analysis and displays results.

Results and Discussions

The analysis is performed using MATLAB as shown in Figure 3.

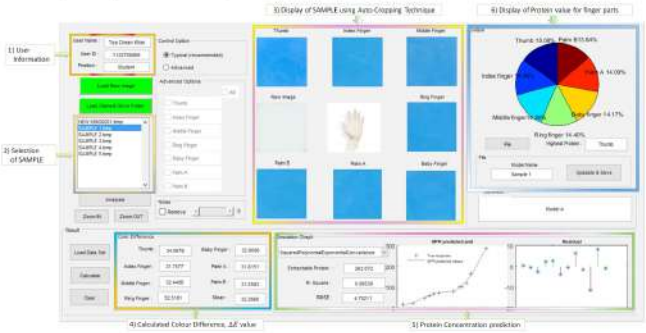

Figure 3: The GUI of Protein Estimation System

A good correlation is formed between the raw protein data provided by the Malaysian Rubber Board (MRB) and the ΔE data as shown in Figure 4. The proposed improvement method is able to simplify the chemical process and reduce the detection time to 1 hour as compared to the Lowry method.

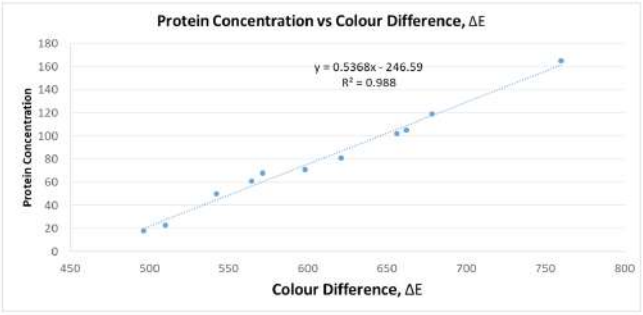

Figure 4: : Protein Assay Data Analysis

Recognitions/ Awards

- ❖ Copyright:
1. CIC/IP/CR/2018-030
2. CIC/IP/CR/2018-011
- ❖ Patent filed:
1. Method and apparatus for colorimetric analysis (PI 2016704027)
2. Latex Article stamping apparatus (PI 2015702206)
- ❖ WSIS 2017 Champion for project "Biocompatibility Platform for Protein Detection in Latex Glove"
- ❖ Merit award at MSC Malaysia APICTA 2014 for the project entitled "Protein Detection with Biocompatibility test in Latex Glove"
- ❖ Testimonial Recognition From Synergy Integrated Resources Sdn Bhd
- ❖ Testimonial Recognition From Deakin University

Linear and Efficient Wideband RF Power Amplifier for Multi-Band Applications

Project leader: Dr. Zubaida Yusoff
Project Member: Assoc. Prof. Dr. Mardeni Bin Roslee
Student : Md. Golam Sadeque
Funding: MMU GRA (MMUI/ 180270.02)
Duration: 15 Sept. 2018 – 14 Sept. 2020

Problem statement

- ❑ A number of amplifiers are used in the base station to cover different frequency bands.
- ❑ Low efficiency and nonlinearity of the RF power amplifier (RF PA).
- ❑ RF PAs are not available in the market for the mid-band frequency range of 3.3 GHz to 4.3 GHz for 5G applications.

Objectives

- ➢ To design broadband Class-F RF PA (1 GHz bandwidth) with high efficiency and good linearity that will replace multiple RF PAs.
- ➢ To fabricate the RF PA using the best components in order to achieve high-performance.
- ➢ To validate the RF PA performance experimentally and compare with the simulation results.

Contribution

1. Wideband RF PA for the upcoming 5G frequency band.
2. Wideband output matching network (OMN) and input matching network (IMN) development using Low Pass Filter Technique (LPFT) and Simplified Real Frequency Technique (SRFT) methods.

Methodology

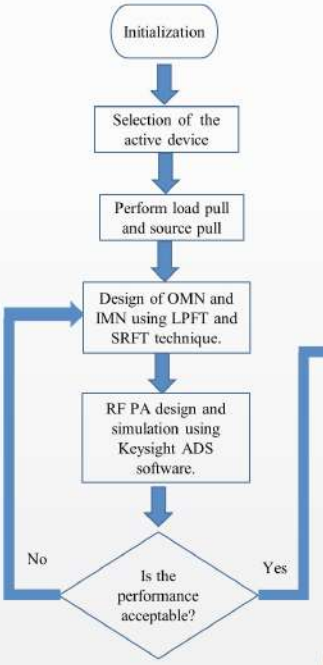

5G Spectrum Allocations

Country	Low Frequency Band (GHz)
USA	3.55 - 3.7
(FCC)	3.7 - 4.2
Finland	3.4 - 3.8
France	3.46 - 3.8
Germany	3.4 - 3.8
Ireland	3.4 - 3.8
Italy	3.6 - 3.8
Russia	3.4 - 3.8
Spain	3.4 - 3.8
United Kingdom	3.4 - 3.6, 3.6 -3.8
China	3.3 - 3.6
Japan	3.6 - 4.2

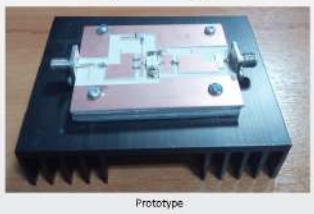

Prototype

Outputs

Conferences

1. M. G. Sadeque, Z. Yusoff, M. Roslee, and N. S. R. Hadi, "Design of a Broadband Continuous Class-F RF Power Amplifier for 5G Communication System," IEEE Reg. Symp. Micro Nanoelectron., pp. 145–148, 2019.
2. A. Fauzi, Z. Yusoff, and M. G. Sadeque, "Inverse Class-F RF Power Amplifier Design Using 10W GaN," 2019 IEEE Reg. Symp. Micro Nanoelectron., pp. 20–23, 2019. (Best paper award)

Journals

1. M. G. Sadeque, Z. Yusoff, and M. Roslee, "A High-Efficiency Continuous Class-F Power Amplifier Design using Simplified Real Frequency Technique," Bull. Electr. Eng. Informatics, vol. 9, no. 5, pp. 1924–1932, 2020. [Scopus Index, Rank: Q2]
2. N. S. R. Hadi, Z. Yusoff, M. G. Sadeque, S. J. Hashim, and M. A. Chaudhary, "High Gain over an Octave Bandwidth Class-F RF Power Amplifier Design using 10w GaN HEMT," Bull. Electr. Eng. Informatics, vol. 9, no. 5, pp. 1899–1906, 2020. [Scopus Index, Rank: Q2]
3. Analysis and Design of the Biasing Network for 1 GHz Bandwidth RF Power Amplifier. (Under process) [Scopus Index, Rank: Q3]

Award:

1. Best paper award at the ICEECC-2019.

Results

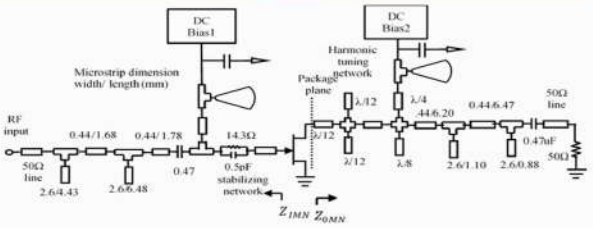

Figure 1: Complete circuit diagram of the proposed RFPA

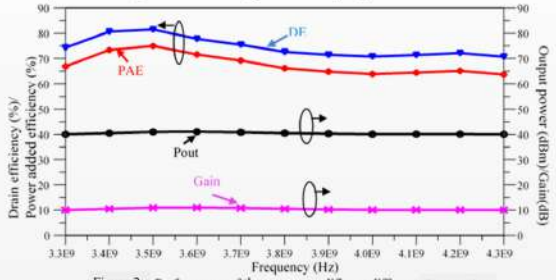

Figure 2: Performance of the power amplifier at different frequencies

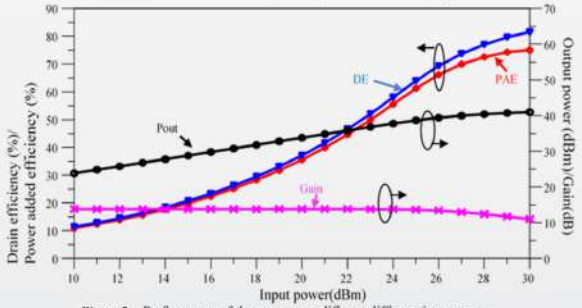

Figure 3: Performance of the power amplifier at different input power.

LTE-DSRC HYBRID PERFORMANCE OPTIMIZATION USING MIMO WITH SPACE TIME FREQUENCY DIVERSITY IN VEHICULAR COMMUNICATION

Hanis Adiba binti Mohamad, Azlan Bin Abdul Aziz, Nur Asyiqin Amir Hamzah, Nor Azlina Ab Aziz, Noor Maizura binti Mohammad Noor

INTRODUCTION

Technology is rapidly growing nowadays and constantly being developed, modified and improved in vehicle-to-vehicle (V2V) communication technology. Therefore, the hybrid model of Long-Term Evolution and Dedicated Short-Range Communications (LTE-DSRC) is designed to provide fast communication, high security between the vehicle with high bandwidth, low latency and high spectrum efficiency. The system is simple to design, deploy and affordable. Therefore, multiple-input multiple-output (MIMO) using 2x2 antennas are adopted to enhance data throughput even under interference, signal fading and multipath conditions using space time frequency block codes (STFBC) diversity technique. This research focuses on physical layer performance of the LTE-DSRC hybrid uplink structure. Simulation of bit error rate (BER), pairwise error probability (PEP) and channel-to-interference ratio (CIR) performances using MATLAB 2019a software simulation are studied. From the results, this proposed method has a significant percentage of improvement of BER and PEP by 56% and 37.1%, respectively.

SIMULATION SET UP AND METHODOLOGY

Figure 1 illustrates the block diagram of the LTE-DSRC hybrid system model transmitter and receiver and Table 1 is system parameter of the S

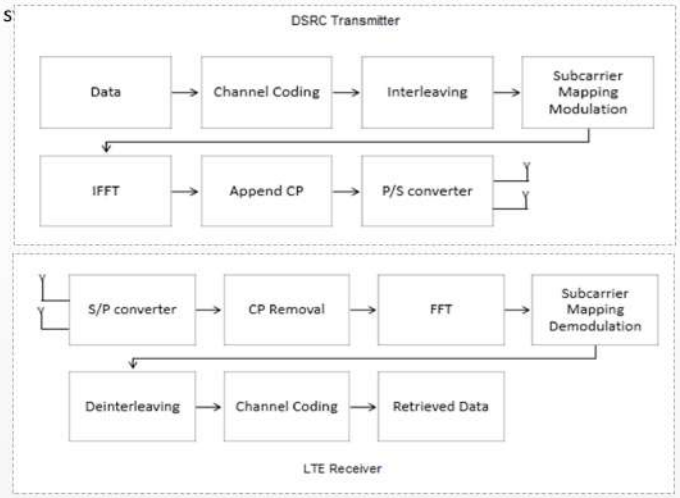

Figure 1: 2X2 MIMO LTE-DSRC hybrid transmitter and receiver

Table 1: LTE-DSRC hybrid system parameter

DFT, IDFT size	64, 1024
Modulation	64 QAM
Bandwidth (MHz)	10
Channel Type	COST 207 Typical Urban
Channel Equalizer	MMSE

RESULTS

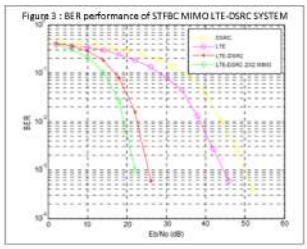

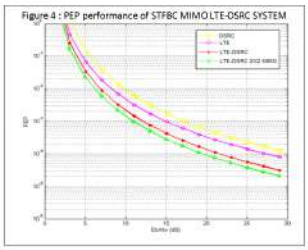

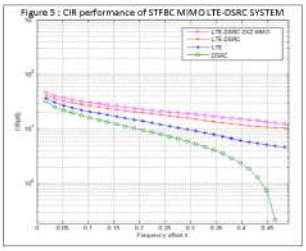

DISCUSSIONS

The results in Figures 3, 4 and 5 suggested that MIMO-LTE-DSRC hybrid system with STFBC outperformed other techniques (i.e., LTE-DSRC, DSRC and LTE) with lower BER value, higher PEP value with higher SNR. Thus, the proposed system achieved maximum frequency diversity gain, less noise and interference with bandwidth efficiency.

CONCLUSION

The proposed method of STFBC diversity in the MIMO LTE-DSRC hybrid vehicular system model outperforms other systems without MIMO, conventional DSRC and LTE systems with 56% and 37.1% of improvement in terms of BER and PEP performances, respectively, which is reliable for vehicular communication system.

ACKNOWLEDGEMENT

This work is supported by TMRND under research grant TMRND MMUE/190012.

REFERENCES

[1] Phidahunlang Chyne, G. Hertkorn, Debdatta Kandar, "LTE-DRSC hybrid vehicular communication System using DFT-spread OFDM uplink,"in International Journal of Communication systems, 27 Aug 2019, volume 32, issue 15, pp. 183-187.
[2] Rezwan, M.S.; Islam, M.A.; Islam, M.M.; Hasan, M.R. Vehicle Breaking Support System. In Proceedings of the 2018 3rd International Conference for Convergence in Technology (I2CT), Pune, India, 6–7 April 2018;pp. 1–4.
[3] ETSI. Intelligent Transport. http://www.etsi.org/technologies-clusters/technologies/intelligent-transport; 2019.
[4] Hu J, Chen S, Zhao L, et al. Link level performance comparison between LTE V2X and DSRC. J Communication Information Network. 2017;2(2):101–112.
[5] Wang X, Ning Z, Hu X, et al. A city-wide real-time traffic management system: enabling crowdsensing in social internet of vehicles. IEEE Communication Mag. 2018;56(9):19–25.
[6] Wang M, Winbjork M, Zhang Z, et al. Comparison of LTE and DSRC-based connectivity for intelligent transportation systems. In 2017 IEEE 85th Vehicular Technology Conference (VTC Spring); 2017:1–5.
[7] Asuzu, P.; Thompson, C. Road condition identification from millimeter-wave radar backscatter measurements. In Proceedings of the 2018 IEEE Radar Conference (RadarConf18), Oklahoma City, OK, USA, 23–27 April 2018; pp. 0012–0016.

Machine Learning-Based Node Selection and jamming strategies Under Physical Layer Security for Cooperative Non-Orthogonal Multi-Access System

>>Mohammed Ahmed Salem, and Azlan Bin Abd.Aziz, Tan Kim Geok, Hadhrami Ab Ghani, Azwan Mahmud, Nur Asyiqin Amir Hamzah, Hatem Al-selwi <<

INTRODUCTION

Non-orthogonal multi access (NOMA) technology is an essential enabler for the fifth generation (5G) wireless networks. The importance of NOMA lies in its ability to serve multi users in a single resource block such as a spreading code, a subcarrier, or a time slot. In this project, We employ the feed forward neural network (FFNN) strategy in order to select the best cooperative node for the relaying or jamming techniques. The proposed approach is compared with another selection approach based on fuzzy logic strategy.

SYSTEM MODEL AND METHODOLOGY

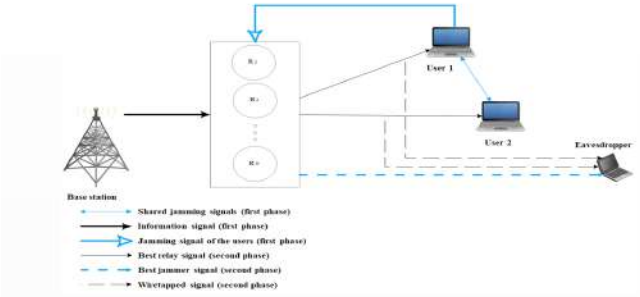

System model

- In first time slot, the base station sends a superimposed information signal to the helper nodes.
- At the same time, $user_1$ and $user_2$ generate jamming signals and share these signals. The shared jamming signals are transmitted by the strong user to the helper nodes.
- In the second time slot, the selected relay amplifies and forwards the superimposed information signal to the user nodes.
- The selected cooperative jammer node directs the shared jamming signal towards the eavesdropper node.
- The eavesdropper wiretaps the main channels in order to receive the transmitted signal from the cooperative relay to the user nodes.

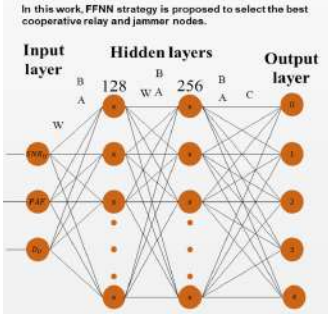

Input Layer [1]-[2]-[3]

The generated relay and jammer data are expressed as,

$$GD_R = [SNR_U, PAF, D_U]^1$$

Hidden Layer [1]-[2].

A (Activation function (ReLu))

$$f_{ReLU}(x) = \max(0, x)$$

B (cost function 250 iterations)

$$L_B(\Theta) = \frac{1}{M}\sum_{i=1}^{M} = -\log\left(o\left(GD_R^i, W, b\right)\right)$$

$$\Theta^{m+1} = \Theta^m - \eta^m \nabla L(\Theta), \text{ where, } \Theta = \{W, b\}$$

C (Activation function (SoftMax))

$$f_{Softmax}(x_i) = \frac{\exp(x_i)}{\sum_{j=i}^{C}\exp(x_j)}$$

The heights probability is considered.

Output Layer [1]-[2]

Illustrates the labelling of cooperative nodes relevance where 0 is very bad, 1 is bad, 2 is medium, 3 is good and 4 is very good

RESULTS AND DISCUSSION

Cooperative relay and jammer nodes selection

Node	Selection criteria						Relevance based on FFNN	Relevance based on FL
	SNR_U	PAF	D_U	SNR_E	D_E	R_S		
1	0.4045	0.7035	0.7538	0.4342	0.6872	True (based on FFNN)	Selected as relay node	
2	0.4357	0.6103	0.7024	0.2176	0.6438	True (based on FL)		Selected as relay node
3	0.3872	0.5200	0.6380	0.0984	0.6009	False		
4	0.3467	0.4345	0.5572	0.0398	0.5588	False		Selected as jammer node
5	0.3125	0.3571	0.4744	0.0146	0.5175	False	Selected as jammer node	

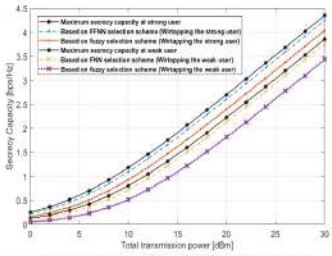

Secrecy Capacity of NOMA Assisted with Smart Node Selection

- Secrecy capacity of the proposed technique and the existing scheme are evaluated with increasing total transmission power.
- The proposed strategy provides high secrecy capacity performance in comparison with the fuzzy logic scheme due to the high estimation accuracy established by the FFNN compared with the fuzzy logic-based selection scheme.

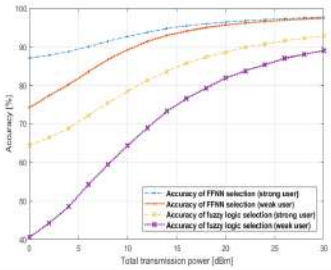

Accuracy analysis for secrecy capacity of the NOMA

- The accuracy analysis is carried out by comparing the maximum secrecy capacity performance of the cooperative NOMA with the resulting secrecy capacity for the proposed node selection based on FFNN and the fuzzy logic-based node selection.

User nodes	Cooperative node selection strategy	
	Fuzzy logic	FFNN
Wiretapping the strong user	0.2639	0.0846
Wiretapping the weak user	0.3343	0.0859

CONCLUSION

In this paper, we proposed a strategy to enhance the physical layer security for a cooperative non-orthogonal multi access system. In conclusion, the results illustrate that the proposed cooperative node selection based on FFNN strategy outperforms the cooperative node selection based on fuzzy logic scheme due to the high estimation accuracy established by FFNN strategy. For future work, it is recommended to consider the assumption of unknown CSI of the eavesdropper node at the base-station and the effect of relay protocols (detect-and-forward, and compress-and-forward) on the secrecy performance analysis.

REFERENCES

[1] Salem, M. A., et al.,"Machine Learning-Based Node Selection and Jamming Strategies Under Physical Layer Security for Cooperative Non-Orthogonal Multi Access System". International Journal on Communications Antenna and Propagation (IRECAP), 2020, Italy.
[2] Salem, M. A., et al.,"Cooperative Relay and Jammer Node Selection Strategies Based on Feed-Forward Neural Network. Accepted by International Conference on Computing and Information Technology (ICCIT-1441), 2020, Saudi Arabia.
[3] T. T. Nguyen, J. H. Lee, M. T. Nguyen, Y. H. Kim,"Machine Learning-Based Relay Selection for Secure Transmission in Multi-Hop DF Relay Networks" Multidisciplinary Digital Publishing Institute (MDPI) on Electronics, vol. 11, no. 1, pp. 239-247, August 2019.

ACKNOWLEDGEMENT

Ministry of Higher Education Malaysia FRGS/1/2019/TK08/MMU/03/1

MULTIUSER MIMO WITH QUANTIZED CSI FEEDBACK

Ivan Ku†, Lee Vei Hung†, Ayman El-Saleh‡, Tuan Anh Le§, and Mohamad Yusoff Alias†

† MMU MULTIMEDIA UNIVERSITY ‡ جامعة الشرقية A' SHARQIYAH UNIVERSITY § Middlesex University

(A) INTRODUCTION

Multiuser Multiple-Input Multiple-Output (MU-MIMO)
It is a technique of transmitting and receiving multiple user data streams simultaneously over the same frequency band.

MU-MIMO challenges:

- Inter-user interference:
  → mitigated using precoders
  → precoder design needs CSI
- Quantized CSI feedback:
  → overhead cost on resources
  → CSI reconstruction accuracy

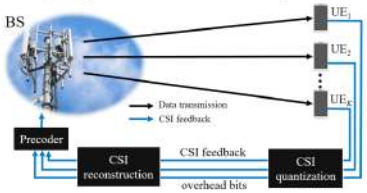

(B) METHODOLOGY

B.1. System Model

Consider a communication system consisting of:
A base station (BS) with N_t antennas and K number of user equipments (UEs). Each UE has N_r antennas.

5 stages of MU-MIMO transmission:

- S1 : BS broadcasts pilot signals, $\mathbf{p}$, to all UEs.
- S2 : All UEs concurrently perform CSI estimation and quantization.
- $S3_k$: Each UE_k sequentially feeds back the quantized CSI, $\hat{\mathbf{H}}_k$, to the BS.
- S4 : Using $\hat{\mathbf{H}}_k$, the BS reconstructs the CSIs of all UEs which will then be utilized in the precoder design for downlink transmission.
- S5 : Data is simultaneously transmitted to all K UEs.

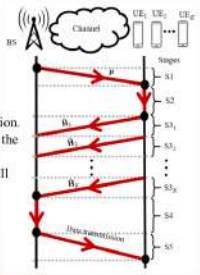

B.2. Effective Transmission Rate

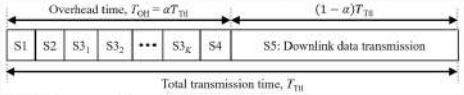

Therefore, the effective transmission rate at each k^{th} UE is

$$R_{eff}^{(k)} = (1-\alpha)R_{BS}^{(k)}, \longrightarrow R_{eff} = \sum_{k=1}^{K} R_{eff}^{(k)}$$

where $R_{BS}^{(k)}$ is the BS downlink transmission rate for the k^{th} UE when using the reconstructed CSI.

B.3. Energy Efficiency

Each stage in the system model consumes power.

The total power consumption, P_{TH}, is the sum of all the power consumed at stages S1 to S5.

Therefore, the energy efficiency is given as $E_E = \frac{R_{eff}}{P_{TH}}$.

(C) SIMULATION PARAMETERS

Assumptions:

- UEs have perfect knowledge of the downlink CSI.
- No noise or distortion on the CSI feedback channel.
- Network operates at full load (K_{max}) at all times.
- Null-space precoder scheme is employed for downlink transmission at stage S5.
- Equal power allocation is employed for the downlink transmission.

TABLE I: Simulation parameters.

Parameter	Value
BS transmit power, P_{BS}	$0 \le P_{BS} \le 46$ dBm
Number of transmit antenna, N_t	$4 \le N_t \le 18$
Number of receive antenna, N_r	2
Maximum number of UEs, $K_{max} = \left\lfloor \frac{N_t}{N_r} \right\rfloor$	$2 \le K_{max} \le 9$
Transmission bandwidth, B_w	20 MHz
Total transmission time, T_{TH}	1 ms
Feedback channel transmission rate, R_0	50% of R_0
BS antenna correlation factor, r_t	0.3
UE antenna correlation factor, r_r	0.3
BS computational power consumption, $\vartheta_{w,BS}$	50 Mfpw
BS computational speed, $\vartheta_{s,BS}$	100 Mfps
UE computational power consumption, $\vartheta_{w,UE}$	100 Mfpw
UE computational speed, $\vartheta_{s,UE}$	50 Mfps
Carrier frequency, f_c	3500 MHz

(D) SIMULATION RESULTS AND DISCUSSIONS

D.1. Various rate metrics

Case 1: Perfect CSI knowledge at the BS

- R_0 is not affected by b and therefore remains constant.
- R_0 is solely dependent on the downlink precoding scheme.

Case 2: Imperfect CSI knowledge at the BS

- For a given downlink precoding scheme, as b increases, the CSI reconstruction accuracy increases and R_{BS} increases towards R_0.
- R_{BS} does not consider the overhead cost in transmitting back b.

Case 3: Imperfect CSI knowledge and overhead cost

- The effective transmission rate, R_{eff}, captures the overhead cost needed to transmit back b, as well as, the effect of imperfect CSI knowledge.
- Although CSI reconstruction accuracy increases at larger b, the increased feedback overhead time, T_{OH}, will far outweigh the former's gain after a certain b threshold, leading to a reduction in effective transmission rate.

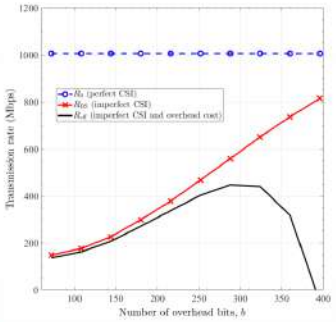

D.2. Energy efficiency and operating points of the network

- E_E follows the profile of R_{eff} as it is proportional to it. That also means P_{TH} is mostly constant as it is dominated by the larger P_{BS} at stage S5 and is less influenced by the varying power consumption at overhead stages S1 – S4 as b varies.
  →Overhead cost more impacted by overhead time, T_{OH}, rather than power consumption of overhead stages S1 – S4.
  →MU-MIMO requires high quality feedback channel to reduce T_{OH} so that optimized R_{eff} becomes nearer to R_0.
- Every R_{eff} has a corresponding E_E, thus, forming an operating point of the network for each b.
- Different sets of $\{R_{eff}, E_E\}$ operating points for the range of b are obtained with different values of N_t and P_{BS}.

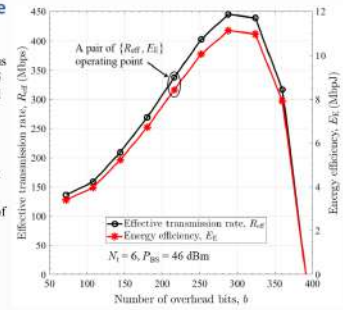

D.3. Rate and energy efficiency trade-off along the Pareto boundary

- As N_t and P_{BS} are varied (Table 1), different sets of $\{R_{eff}, E_E\}$ operating points are obtained.
- These operating points form the eTREE region (yellow area).
- The outermost eTREE boundary is where all the optimized network operating points are located.
- Multi-objective particle swarm optimization (MOPSO) is used to verify this outermost eTREE boundary.
  - When conflicting objectives are present, MOPSO generates a Pareto boundary where all Pareto efficient solutions are located.
  - Along this boundary, any one objective cannot be continuously improved without the expense of the other, that is, a trade-off exists.
- The Pareto boundary matches the outermost eTREE boundary.
  - This boundary is where all the optimized $\{R_{eff}, E_E\}$ pairs are located.
  - A trade-off exists among the optimized $\{R_{eff}, E_E\}$ pairs.

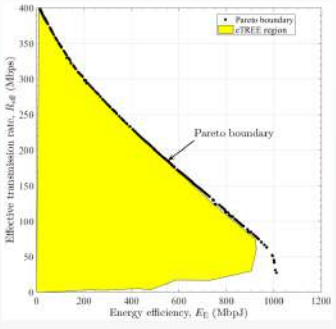

(E) CONCLUSIONS

- A MU-MIMO network with quantized CSI feedback is presented whereby the importance of incorporating the additional overhead incurred during CSI feedback into the performance metrics is highlighted.
- Trade-off between the optimized effective transmission rate and energy efficiency of the MU-MIMO network is demonstrated by the Pareto boundary of a multi-objective particle swarm optimization.

(F) PUBLICATIONS

[1] V. H. Lee, I. Ku, A. A. El-Saleh, and T. A. Le, "On the efficiency of MIMO transmission with channel state information feedback," in *Proc. ICT'19*, Hanoi, Vietnam, Apr. 2019.
[2] V. H. Lee, I. Ku, A. A. El-Saleh, T. A. Le, N. I. A. Razak, and M. Y. Alias, "Performance of practical multiuser MIMO networks with limited CSI feedback" in *Proc. IEEE MICC'19*, Selangor, Malaysia, Dec. 2019.
[3] I. Ku, V. H. Lee, A. A. El-Saleh, A. L. Tuan, and M. Y. Alias, "Trade-off performances in multiuser MIMO networks with quantized CSI feedback," in *Proc. IEEE ISTT'20*, Selangor, Malaysia, Nov. 2020 (**Best Paper Award**).

PEAK-TO-AVERAGE POWER RATIO (PAPR) REDUCTION TECHNIQUES FOR VISIBLE LIGHT COMMUNICATION

PROF. DR. MOHAMAD YUSOFF BIN ALIAS, FACULTY OF ENGINEERING, MULTIMEDIA UNIVERSITY

Abstract

This work proposes a new hybrid scheme to decrease the high peak-to-average power ratio (PAPR) of optical orthogonal frequency division multiplexing (OFDM) signals in visible light communication (VLC) systems. The proposed method is applicable for both direct current-biased optical OFDM (DCO-OFDM) and asymmetrically-clipped optical OFDM (ACO-OFDM). In the proposed scheme, the PTS method is firstly modified to fit both optical OFDM approaches for transmission and then combined with signal clipping method for further PAPR reduction and bit error rate (BER) improvement of the VLC system. The performance of hybrid scheme has been evaluated and compared with the original OFDM based VLC system, conventional PTS and clipping methods.

Methods

This work proposes a new and hybrid scheme for reducing the PAPR of OFDM signals in VLC system using combined PTS and signal clipping techniques as shown in Figure 1. In the proposed hybrid scheme, the PTS method is modified to be suitable for VLC transmission and then combined with signal clipping method for further improvements in both the PAPR reduction and BER performance of the VLC system.

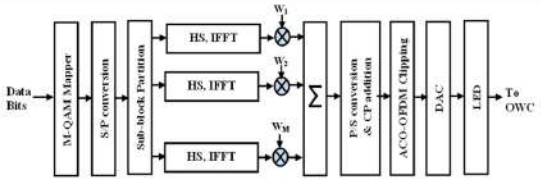

Figure 1: Block diagram of the proposed scheme for ACO-OFDM VLC

Results

The performance of ACO-OFDM in VLC system is analyzed in term of PAPR reduction and BER performance. The simulation results of the signal clipping, PTS algorithm and the proposed hybrid scheme, are evaluated and compared. The simulation uses MATLAB software.

Discussion

Figure 3 shows that the proposed hybrid scheme for ACO-OFDM has a slightly lower PAPR (0.1 dB reduction gain) as compared to DCO-OFDM around CCDF of 10−1. Figure 4 shows, for higher SNR values (beyond 13 dB), DCO-OFDM outperforms ACO-OFDM because of spectral efficiency.

Conclusions

Comparing with other methods, the PAPR reduction gain of the proposed method is about 5.5 dB and 1 dB compare to the signal clipping and the modified PTS method, respectively.

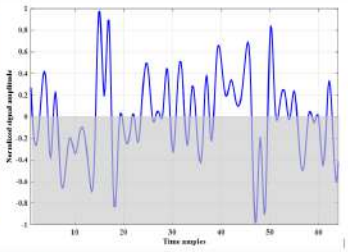

Figure 2: ACO-OFDM time domain signal. The clipped negative values are in shaded area.

Acknowledgements

This work is supported by the Telekom Malaysia Research & Development Residual Grant under project number MMUE170010.

Knowledge Transfer

Tutorial Session at The 7th International Conference on Smart Computing and Communication (ICSCC 2019) Curtin University Malaysia Miri, Sarawak, Malaysia, 28 June 2019

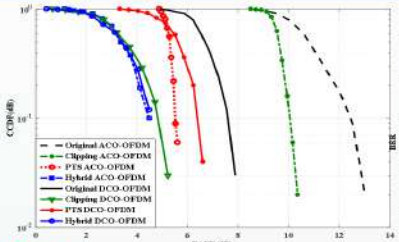

Figure 3: The CCDF comparison of ACO-OFDM and DCO-OFDM with different approaches

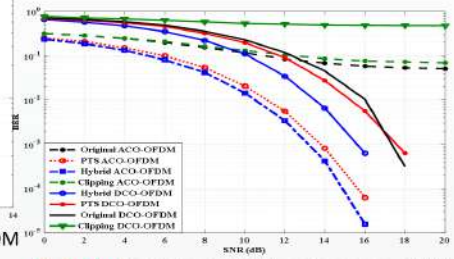

Figure 4: Comparison of BER performance of ACO-OFDM and DCO-OFDM with different approaches

Journal papers

1. A. A. Abdulkafi, Y. S. Hussein and M. Y. Alias, "Recursive Clipping for Channel Estimation in VLC Systems," Solid State Technology Journal, vol. 63, no. 2s, pp. 3069-3077, 2020.
2. Touhami, R., Slimani, D., Abdulkafi, A., Y. S. Hussein, M. Y. Alias (2020). Combined Envelope Scaling with Modified SLM Method for PAPR Reduction in OFDM-Based VLC Systems . Journal of Optical Communications, 0(0), pp. -. Retrieved 27 Feb. 2020, from doi:10.1515/joc-2019-0273
3. Y. S. Hussein, M. Y. Alias, A. A. Abdulkafi, N. Omar and M. K. Salleh," Expectation Maximization Based Channel Estimation Algorithm for OFDM Visible Light Communication Systems," International Journal of Engineering & Technology, vol. 7, no. 4, pp. 2638-2645.
4. A. A. Abdulkafi, M. Y. Alias, Y. S. Hussein, N. Omar and M. K. Salleh, "A Hybrid PAPR Reduction Scheme for Optical Wireless OFDM Communication Systems," KSII Transactions on Internet and Information Systems, vol. 12, no. 3, pp. 1136-1151, 2018.

Collaborators

1. **Post-doc:** Dr. Ayad Atiyah Abdulkafi, Electrical Engineering Department, Tikrit University, Salahaddin, Iraq
2. **Post-doc:** Dr. Yaseein Soubhi Hussein, Department of Information Systems and Computer Science, Ahmed Bin Mohammed Military College, Qatar
3. **Exchange researcher:** Ridha Touhami, University of Ferhat Abbas Setif 1, Setif 19000, Algeria.

References

Awards

Best Paper Award at the 2017 IEEE 13th Malaysia International Conference on Communications (MICC) for the paper "PAPR Reduction of DC Biased Optical OFDM using Combined Clipping and PTS Techniques"

Conference papers

3 conference papers.

REAL-TIME OPTICAL FIBER DOSIMETRY SYSTEM

Founder : Prof. Ir. Dr. Hairul Azhar Bin Abdul Rashid
Co-founder: Md. Zubair Hassan Tarif.
Affiliation: MULTIMEDIA UNIVERSITY, CYBERJAYA.

OVERVIEW

Ionizing radiation technology is useful in many applications ranging from medical to industrial applications. One of the important aspects of this technology is measurement of the absorbed dose, particularly in medical applications such as Radiotherapy. Despite the available technologies to measure the absorbed dose, there are many setbacks in addressing accuracy and speed. To facilitate reliable, reproducible, and accurate readings in real time the sensing material must be able to maintain constant level of luminescence (usually quantified by photon counts) consistently at a particular dose rate. The luminescence must also be linearly proportional to changing dose rates. An optical fiber based doped silica RL dosimeter (with accompanying PC-based software) has been developed to accomplish the aforementioned tasks.

THE INVENTION

The LS1000 is a real-time radiation dosimeter that is specially designed for small-field radiotherapy applications used in IMRT, Radiosurgery, SRS and IGRT. Based on a custom-made optical fiber, the LS1000 is able to measure absorbed dose from small-field radiation accurately and instantaneously

Market Potential

The market segmentation of the developed dosimeter is shown above. From a market research report (n-tech), the total demand for dosimeters is expected to be about USD 522 mil. by year 2022.

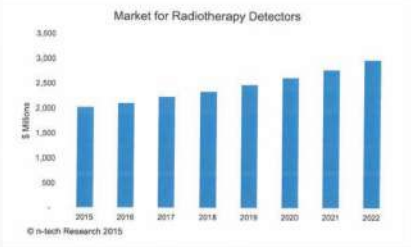

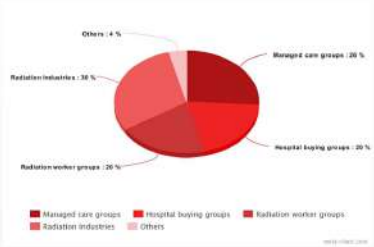

Competitive Advantages

- ❑ Real Time Monitoring: The fiber dosimeter is connected directly to the LS1000 Dosimetry System, allowing instantaneous measurement.
- ❑ Remote monitoring: The fiber dosimeter can be connected to a long transmission fiber (up to 30m), allowing remote monitoring.
- ❑ Impervious to water: The doped silica optical fiber used as the dosimeter is impervious to water, allowing in-vivo measurements to be made.
- ❑ Free from Electromagnetic Interference: The fiber dosimeter operates in the optical domain, hence no electromagnetic interference.

Life Made Easier™ | TM Group

Rehabilitation Using Biofeedback System

K.S. Sim, K.L. Lew, C.C. Lim, F. Sammani, M. Alsayed
Faculty of Engineering and Technology, Multimedia University, Melaka

Introduction

Rehabilitations are conventionally done in hospitals and are time-consuming for the patients. The patients do not feel motivated as they have to travel to the hospitals from their home. The proposed system is a **home-based, virtual reality rehabilitation** application, embedded with biofeedback. The patients can choose any rehabilitation activity at home without the need for on-site supervision by a medical caregiver. There are 4 activities programmed into the application: **Pick and place**, **Mirror Pick and place**, **Wall Climbing**, and **Hit the ball**. Each of the activities is designed for rehabilitation of **upper limb motor function**.

Objectives

- To design and develop a biofeedback system
- To design a virtual reality environment for rehabilitation
- To design and develop rehabilitation activities using virtual reality

Proposed System

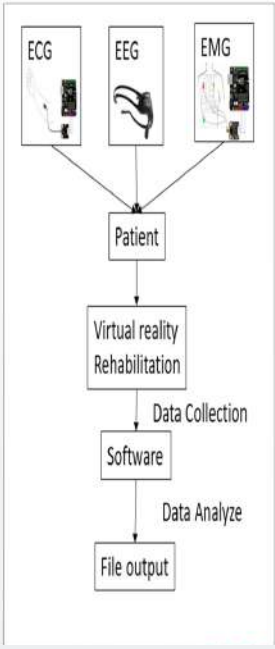

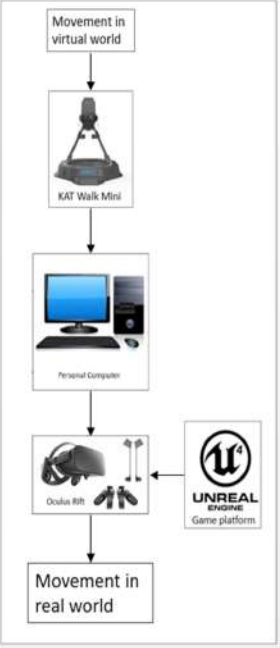

Project Outcome

Before starting rehabilitation exercises, the patient is required to undergo an **ECG test** to check the condition of the patient's heart.

There are **4 activities** in the application:

Throughout the rehabilitation activities, the patient is required to wear the **EEG headset** and **EMG sensor** to monitor brain wave and muscle power. Muscle power is an indicator of improvement in stroke patient.

Recognition & Award

- **Copyright**

1. CIC/IP/CR/2019-032
2. TTO/IP/CR/2020-024
3. TTO/IP/CR/2020-047
4. TTO/IP/CR/2020-023
5. TTO/IP/CR/2020-049
6. TTO/IP/CR/2020-037

- **Patent**

1. PI 2012004764
2. PI 2019006481

- **Collaboration with**

1. Chiba University
2. Hospital Melaka
3. Universiti Kebangsaan Malaysia
4. Perkeso Melaka

- **Publications**

1. K. S. Sim et al. (2019). Development of Dementia Neurofeedback System using EEG Brainwave Signals. *IJSPS*, 7(4), 113-117.
2. K. S. Sim et al. (2019). Deep Convolutional Networks for Magnification of DICOM Brain Images. *IJICIC*, 15(2), 725-739.
3. S. Fawaz et al. (2020). Encoding Rich Frequencies for Classification of Stroke Patients EEG Signals. *IEEE Access*, 8, 135811-135820.
4. K.L. Lew et al. (2020). 3D Kinematic of Upper Limb Functional Assessment Using HTC Vive in Unreal Engine 4. *ICCCI*, 264–275.
5. C. C. Lim et al. (2021). Determination of Muscle Power Using RMS of Electromyography for Stroke Survivors, *ICISA*, 201-210.

REINFORCEMENT LEARNING FOR ROBOTIC APPLICATIONS USING DEEP CNN AND IoT

Hatem Fahd Al-Selwi, Azlan Bin Abd.Aziz, Fazly Salleh Abas,
Azwan Mahmud, Nur Asyiqin Amir Hamzah

INTRODUCTION

Reinforcement learning (RL) enables robots to perform complex tasks with less amount of control engineering [1]. However, using reinforcement learning in robotic applications is challenged by several problems such as high dimensionality. Thus, this project studies the implementation of the Hindsight Experience Replay (HER) algorithm in integration with deep conventional neural network to reduce the dimensionality of the problem the RL is learning to solve [2]. Moreover, the efficiency of RL in factories can be improved by using IoT systems to distribute the learned policies between all connected (agents) robots. Therefore, all agents can make use of the learned policy by any one of the agents.

SETUP AND METHODOLOGY

Figure 1 illustrates the setup required to train and share the learned policy to all connected robots.

.

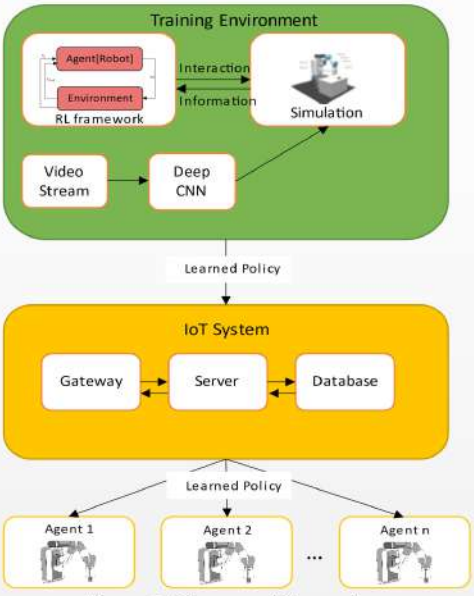

Figure 1: Diagram of the system

In this research, the system was tested on a simulated environment using 7-DoF robot on Mujoco simulator.

SIMULATION RESULTS

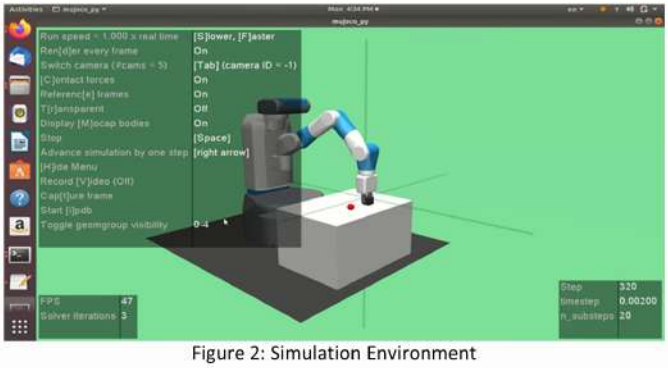

Figure 2: Simulation Environment

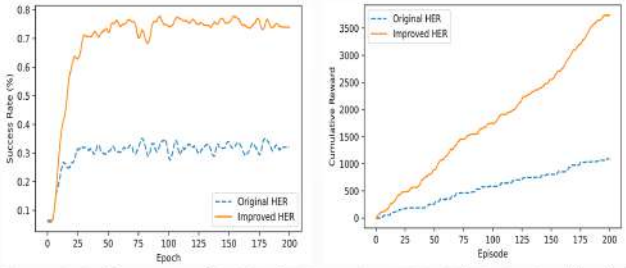

Figure 2: Performance of Original HER against HER with Vision Feedback. [2]

Table 1: Performance Matrix .

Method / Object	Original HER (success rate)	HER with the vision feedback (success rate)	Efficiency
Cubic Object	98%	98%	0%
Cuboid Object	30.9%	80%	61.37%
Complex Object	50%	50.2%	0.4%

CONCLUSION

This research offers a framework for more efficient control systems for robots where robots learn a policy of how to preform complex tasks without being explicitly programed for them. Moreover, the use of CNN gives more generality for the object being manipulated. The learned policy can be shared with other robots connected to the IoT system. Therefore, the time needed for learning certain tasks is reduced accordingly .

REFERENCES

[1] R. S. Sutton and A. G. Barto, Reinforcement Learning: An Introduction, Second. The MIT Press, 2018.

[2] M. Andrychowicz et al., "Hindsight experience replay," Adv. Neural Inf. Process. Syst., vol. 2017-Decem, no. Nips, pp. 5049–5059, 2017.

Acknowledgement

Project is supported by TMRND MMUE/190012

RESPONSE SURFACE MODELLING OF 3D PRINTED ALUMINIUM PART

Low Keen Wei, Dr. Chockalingam Palanisamy

Introduction

3D printing is one of the most innovative manufacturing methods. The objective of the study is to develop a Response Surface Model (RSM) to predict the tensile strength, hardness, and compression strength of 3D printed Aluminium-Polylactic Acid (Al-PLA) specimens.

Methods & Materials

A Response surface model developed was developed using Central Composite Design (CCD) of Design of Experiment (DOE). Sets of control input parameters and response surface design are shown in Table 1 and Table 2. 15 sets of Al-PLA specimen were 3D printed using MakerBot Replicator 5th Generation 3D Printer (Fig. 1). Three mechanical testing which are tensile testing, hardness testing, and compression testing were conducted on the AL-PLA specimen.

Table 1 Input Parameters

Parameter	Levels		
	-1	0	1
Layer Thickness (mm)	0.1	0.2	0.3
Infill Density (%)	20	40	70
Number of Shells	2	3	4

Table 2 Response Surface Design

Test Number	Coded values			Actual Values		
	Layer Thickness	Infill Density	Number of Shells	Layer Thickness (mm)	Infill Density (%)	Number of Shells
1	-1	-1	-1	0.1	20	2
2	1	-1	-1	0.3	20	2
3	-1	1	-1	0.1	70	2
4	1	1	-1	0.3	70	2
5	-1	-1	1	0.1	20	4
6	1	-1	1	0.3	20	4
7	-1	1	1	0.1	70	4
8	1	1	1	0.3	70	4
9	-1	0	0	0.1	40	3
10	1	0	0	0.3	40	3
11	0	-1	0	0.2	20	3
12	0	1	0	0.2	70	3
13	0	0	-1	0.2	40	2
14	0	0	1	0.2	40	4
15	0	0	0	0.2	40	3

Figure 1 MakerBot Replicator

Results & Discussion

The results obtained from the mechanical testing are shown in Table 3(a), (b) and (c). All the results obtained from the mechanical testing were then fed into Minitab Software to develop the Response Surface Model of the Al-PLA specimen. Regression equation is obtained from the software to compute the theoretical data. The percentage of difference for the 15 specimens for each mechanical testing is below 5% which is desirable. In order to prove the validity, 6 new parameters of Al-PLA specimens were printed and the results are tabulated in Table 4a, Table 4b and Table 4c. Since the percentage of difference for all outputs of the mechanical testing are less than 5%, the Response Surface Model of Al-PLA specimen developed is valid.

Table 3 Test Results (a) Tensile (3) Hardness (c) Compression

Sample No.	Layer Thickness (mm)	Infill Density	Number of Shells	Tensile Test (kN)	Hardness Test	Compression Test (kN)
1	0.1	0.2	2	0.934	72.2	14.9
2	0.3	0.2	2	0.898	75.4	15.3
3	0.1	0.7	2	1.068	77.6	16.1
4	0.3	0.7	2	1.005	80.2	16.4
5	0.1	0.2	4	0.965	76.7	18.2
6	0.3	0.2	4	0.905	77.4	18.6
7	0.1	0.7	4	1.087	83.8	19.5
8	0.3	0.7	4	1.056	86.4	20
9	0.1	0.4	3	0.979	76.5	17.2
10	0.3	0.4	3	0.924	77.9	18
11	0.3	0.2	3	0.965	74.9	16.9
12	0.2	0.7	3	1.008	85.4	18
13	0.2	0.4	2	0.956	75.5	16.2
14	0.2	0.4	4	0.985	82.9	18.8
15	0.2	0.4	3	0.971	79.4	17.5

Table 4 Validity Experiment Specimens Test Results (a) Tensile (b) Hardness (c) Compression

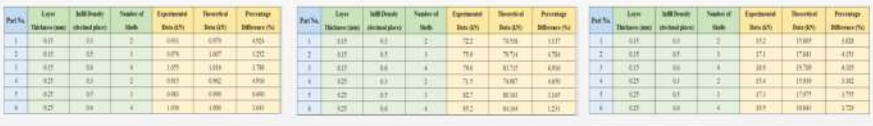

Conclusion

The objective of this study which is to develop a Response Surface Model to predict the mechanical properties of Aluminium-PLA specimens from sets of control input 3D printing parameters variation was successfully achieved. Further mechanical testing is recommended to conduct in order to have more precise and persuasive data to prove that the developed Response Surface Model is valid.

TRACKING LOCALIZATION IN SMART BINS USING LOAD CELLS

Sedia Jaiteh (1122702512@student.mmu.edu.my)
Supervisor: Dr. Tan Ching Seong (cstan@mmu.edu.my)
Co-Supervisor: Ir. Dr. Lini Lee (linilee@mmu.edu.my)

Introduction

Localization is the concept of estimating the location of an object or in our case, the human foot. This concept has broad applications in radar, sonar, security and biometric tracking systems. In this work, location estimation is used to perform human gait analysis from force reactions by focusing on (x-coordinate, y-coordinate) on a force platform. Heel strike, toe strike and the subsequent distance between them on the force platform were considered for analysis and gait recognition. Conventional biometric inputs like finger prints require bodily contact, human iris requires proximity to the sensor and facial recognition requires both proximity and a good light source. These limitations can be addressed by using human gait as an input on a force platform. There are mainly two types of gait analysis sensor designs with relation to ground reaction force: force plate and custom footwear. The latter is often a shoe fitted with sensors and the former will be presented in this work.

Prototype Description

The prototype presented in this paper uses four load cells as its primary input sensors. The load cells are connected to the processing board, which can communicate with an android device through an built-in Bluetooth module. For the most part, load cells are used to measure weight or force changes and, due to their range of sensitivity, they can measure things as small as a needle to as heavy as a drilling machine. The processing board contains multiple components: an SD card module, multiple HX711 amplifiers, a Bluetooth 4.0 (BLE) module, a power port and an Arduino micro pro. The prototype is power-efficient and can run on solar energy. The mathematics involved in this work would utilize the weight readings from the load cells and the distance between them. The force platform is a metal square-shaped platform with an area of about $1m^2$.

Objectives

- To estimate location on a force platform.
- To investigate the limitations of position estimation.
- To implement localization technique for human gait analysis.
- To explore the use of load cells as primary sensors for data collection and location estimation.
- To explore X and Y localization technique on force platforms.

Flow

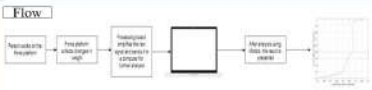

Problem formulation

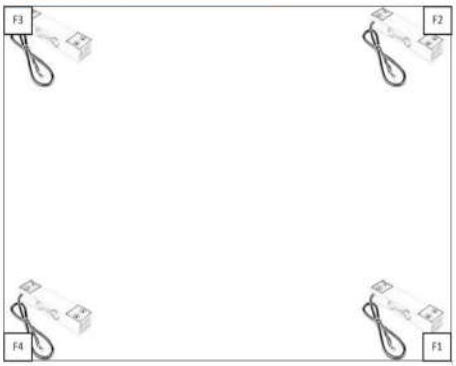

(x-coordinate, y-coordinate)

- Four load cells attached under the four corners of the force platform.
- This platform can be viewed as an x-y graph with any corner being the reference.
- When a human walks on the platform, the load cells records the changes of weight placed on them.
- These changes are sent to the processing board through the hx711 amplifier.
- In the following equations: W stands for the weight placed on the platform, F_i represents the resultant forces from the four load cells. x and y represents the (x-coordinate, y-coordinate) and L represents the length of the force plat form, which is $1m$.
- F_i unit is in KG and L is in meters.

$$-\vec{F} = \sum_{i=1}^{4} x\vec{W} \quad -(\vec{r}\times\vec{F}) = \sum_{i=1}^{4}(\vec{r}\times\vec{W}) \quad \rightarrow \quad -(\vec{r}\times\vec{F}) = \sum_{i=1}^{4}(\vec{r}\times\vec{W}) \quad \rightarrow \quad x\times F = (F_2+F_3)L \quad y\times F = (F_3+F_4)L \quad \rightarrow \quad x = \frac{(F_2+F_3)L}{\sum_{i=1}^{4}F_i} \quad y = \frac{(F_3+F_4)L}{\sum_{i=1}^{4}F_i}$$

Table 1

F_1	F_2	F_3	F_4	W	x	y
10.541	4.992	0.4310	1.5210	17.4850	0.3102	0.1116
24.3210	21.619	4.7820	4.8310	55.5530	0.4752	0.1730
20.503	20.914	6.0150	5.3010	52.733	0.5107	0.2146
20.5710	20.614	9.219	7.7260	58.13	0.5132	0.2915
11.4080	18.81	19.1360	16.1370	65.491	0.5794	0.5386
2.6700	2.793	35.5860	26.2100	67.2590	0.5706	0.9188
1.149	0.6530	29.7380	21.3720	52.9120	0.5744	0.9659
0.632	0	27.4330	13.6060	41.6710	0.6583	0.9848

- Table 1 shows the multiple weights recorded at all four load cells as a person walks on the force platform. Every row contains individual weight readings at each load cell per activity, the total weight from all load cells and the resultant x-coordinate and y-coordinate were computed from the relationships in the problem formulation section.
- This location estimation can be used to determine when a person's heel or toe is active on a force platform and the location of that particular heel from the next heel or toe.
- This table in its totality is specific to one person due to the uniqueness of human gait.
- Figure 1 shows the resultant graph and pattern of movement collected from a subject. Every (x,y) coordinate represents a change in reaction force, with the first four representing the right foot and the last four points representing the left foot. The changes in forces are in a heel-strike followed by toe-strike sequence.

Processing Board

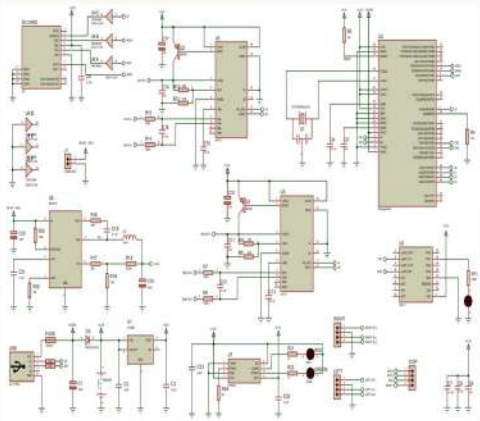

Components

- HX711 Amplifier amplifies the data from the load cells
- ATmega32U4 is the central MCU
- SD card module for data storage
- U8 is the BLE module for data transfer to an android device
- CC2541 Low Energy Bluetooth

Specification

- Power: 3.7V @ 0.9μA in ideal state and 35mA in active state.
- Can be powered: 6V Solar panel charging at 200mA to 500mA (depending on the weather)
- Data logging with up to 32GB microSD
- Low power consumption
- Support self-sensor calibration and manual calibration

Figure 1

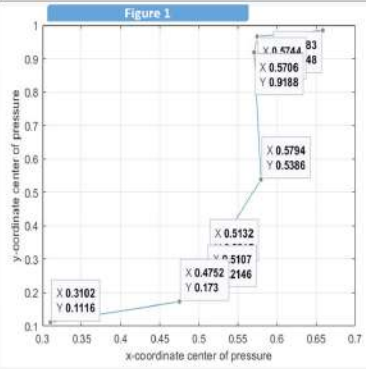

Conclusion

This prototype has four load cells attached to each corner to monitor human movement on the force platform. The force platform is connected to a processing board where data is collected and stored. The x-coordinate , y-coordinate calculation and analysis was done with MATLAB. Human gait recognition was possible using the distances between subsequent heel and toes strikes, the distance between them using (x,y) localization technique. The relationships derived in the problem formulation section were acceptable because the error margin between the calculated and measured (x,y) coordinates differ by less than 5%.

VISCOUS DISSIPATIVE FORCED CONVECTION IN POROUS MEDIUM

Mirza Farrukh Baig, Chen Gooi Mee, Tso Chih Ping
Centre for Advanced Mechanical and Green Technology (CAMGT), Faculty of Engineering and Technology,
Multimedia University, Melaka, Malaysia.

Introduction

- Porous medium is widespread in engineering applications for heat transfer enhancement.
- Viscous dissipation, as form of heat source comprising of internal and frictional heating, has an adverse effect on the heat convection from a heated boundary.
- This study evaluates the effect of viscous dissipation a porous medium.

Methods of Investigation

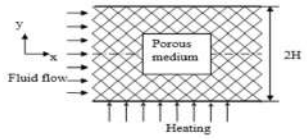

Fig. 1. Schematic Diagram of the problem (Adapted from [1])

Objectives

- To compute the fluid and solid temperature distribution in a channel subjected to heating on one side, saturated with the porous medium under Local Thermal Non Equilibrium (LTNE) condition.
- To investigate the effect of viscous dissipation on the convection heat transfer coefficient.

The governing thermal energy equations for the porous medium, are [1]:

$$k_{s,eff}\frac{\partial^2 T_s}{\partial y^2} - h_i a_i = 0 \quad (1)$$

$$k_{f,eff}\frac{\partial^2 T_f}{\partial y^2} + h_i a_i (T_s - T_f) + \frac{\mu_f}{K}{u_p}^2 + \mu_{eff}\left(\frac{\mathrm{d}u_p}{\mathrm{d}y}\right)^2 = \rho_f c_{p,f} u_p \frac{\partial T_f}{\partial x} \quad (2)$$

The following dimensionless variables are introduced

$$\theta = \frac{k_{s,eff}(T - T_w)}{q_w H}, Bi = \frac{h_i a_i H^2}{k_{s,eff}}, \kappa = \frac{k_{f,eff}}{k_{s,eff}},$$

$$Br = \frac{\mu_f {u_m}^2 H}{q_w K}, Da = \frac{K}{H^2}, S = \frac{1}{\sqrt{MDa}} \quad (3)$$

Dimensionless energy equations for the parallel plates subjected to bottom heating are solved to get the temperature fields.

Results and Discussion

- The variations of internal heating (I.H) and frictional heating (F.H) for different porous medium shape factors, S with the transverse direction are plotted in Fig. 2(a) and (b).
- In Fig. 2(a), when $S = 1$ the sum of I.H and F.H rises to a higher value at the vicinity of the walls, and F.H is more dominant than I.H near the boundary.
- When S increases to 30 in Fig. 2(b), the sum of viscous dissipation is uniform except for a very thin boundary layer near the wall.
- The two-dimensional temperature line plots shows viscous dissipation has a profound effect on a microchannel heat sink, as shown in Fig. 3(a) and (b).

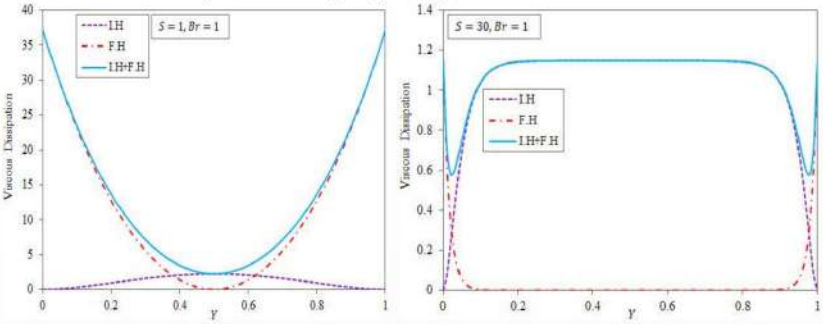

(a) (b)

Fig. 2. Viscous dissipation in the channel (a) $S = 1, Br = 1$ (b) $S = 30, Br = 1$

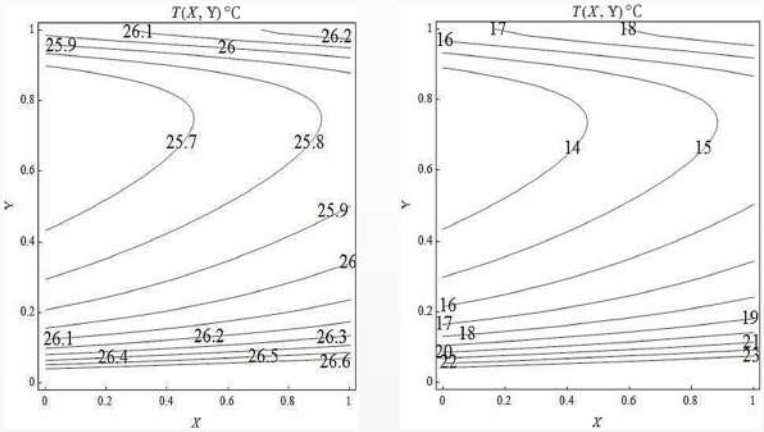

(a) (b)

Fig. 3 Fluid Temperature Line plots (a) $q_w = 20 \times 10^4$ W/m², $S = 10\sqrt{5}, Br = 0.6418$ (b) $q_w = 200 \times 10^4$ W/m², $S = 10\sqrt{5}, Br = 0.0641$

Conclusion

Viscous dissipation as a form of heat generation has a profound effect on the temperature distribution, for a lower heat flux in particular.

Acknowledgements

The authors would like to acknowledge Multimedia University gratefully for funding this research under internal GRA grant, MMUI/170126.02.

1. O.M. Chen, C.P. Tso, Forced convection with viscous dissipation using a two- equation model in a channel filled by a porous medium, International Journal of Heat and Mass Transfer 54 (2011) 1791-1804.

ACKNOWLEDGEMENT

RICES 2020 Organising Committee

Units related:
All MMU Faculties
Entrepreneur Development Centre (EDC)
President's Office
VP Marketing & Communication Office
Corporate Communications Unit
IT Services Division (ITSD)
MMU Production Team
Multimedia Product Innovation Unit
Media Support Unit
Facilities Management Department
Procurement Unit
MMU Staff Development Committee

e ISBN 978-967-19560-3-8